ADDIS ABABA UNIVERSITY

ADDIS ABABA INSTITUTE OF TECHNOLOGY

SCHOOL OF CIVIL AND ENVIRONMENTAL ENGINEERING

EFFECT OF LOSS OF BOND ON THE SHEAR BEHAVIOR OF SHORT REINFORCED CONCRETE BEAM

A Thesis in Structural Engineering

By Asseged Tesfaye

22/01/2012

Addis Ababa

A Thesis

Submitted in Partial Fulfillment of the Requirements for the Degree of Master of Science

The undersigned have examined the thesis entitled '**EFFECT OF LOSS OF BOND ON THE SHEAR BEHAVIOR OF SHORT REINFORCED CONCRETE BEAM**' presented by **Assegid Tesfaye**, a candidate for the degree of **Master of Science** and hereby certify that it is worthy of acceptance.

Dr. Esayas Gebreyohannes		
Advisor	Signature	Date
Internal Examiner	Signature	Date
External Examiner	Signature	Date
Chair person	Signature	Date

UNDERTAKING

I certify that research work titled “Effect of Loss of Bond on The Shear Behavior of Short Reinforced Concrete Beam” is my own work. The work has not been presented elsewhere for assessment. Where material has been used from other sources it has been properly acknowledged / referred.

Asseged Tesfaye

ABSTRACT

Bond between concrete and reinforcement is the major factor for load transfer from the bar to the concrete. The shear flow in reinforced concrete beams depends on the existence of this bond. In this paper shear behavior of a reinforced concrete beam, with different unbonding length, is studied. The effect of loss of bond on the shear capacity and the crack pattern of RC beam has been examined. In order to discover the ultimate shear strength, four reinforced concrete beams with partially unbonded length were tested and simulated with Vector FormWork 4.3 software. The partially unbonded length were the parameter. Results from experiment and software showed that for the increment of unbonding length, the ultimate shear capacity increases and the crack pattern varies.

Keywords: Shear behavior, Partial length, Unbond

ACKNOWLEDGMENTS

First of all I would like to thank the almighty GOD for being there in all hard times I have been through. My adviser, Dr Esayas Gebreyohannes, I am very grateful for your invaluable support, encouragement, guidance and valuable advice during my program of study. This thesis would not have been possible without your direction & support.

I would also like to thank my friends Mr Birhanu Legesse and Mr Natnael Engdasew for their support during laboratory work. Last but not least my thanks goes to my dearest family who were helpful along the way and make me feel strong when I gave up on things.

TABLE OF CONTENTS

LIST OF TABLES

LIST OF FIGURES

CHAPTER 1 INTRODUCTION

1.1 Background

In the design of a reinforced concrete member, flexure is usually considered first, leading to the size of the section and the arrangement of reinforcement to provide the necessary moment resistance. Limits are placed on the amounts of flexural reinforcement which can be used to ensure that if failure was ever to occur, it would develop gradually, giving warning to the occupants. The beam is then proportioned for shear. Unlike flexural failures, reinforced concrete shear failures are relatively brittle (do not undergo significant plastic deformation) and, particularly for members without stirrups, can occur without warning. The manner in which shear failures can occur varies widely with the dimensions, geometry, loading, and properties of the members. So as suggested by the damage sustained by the building the design for shear must ensure that the shear strength equals or exceeds the flexural strength at all points in the beam.

Reinforced concrete structures could deteriorate and fail to serve the intended function due to several adverse effects, among those, loss of bond between reinforcement steel and plain concrete is one. The existent of bond in RC has a significant role in resisting loads through transfer of stress from the steel to concrete. In a reinforced concrete beam, the flexural compressive stress is resisted by concrete, while the tensile one is by reinforcing steel. For this process to exist, there must be a force transfer or bond, between the two materials. The forces along the reinforcing bar is equilibrated by the existence of bond stresses. Bond stress is defined as the transfer of stress loads across the interface between the concrete and reinforcement bars. It represents the interaction between the steel reinforcement and the surrounding concrete. The primary mechanism of bond is the mechanical interlocking between the concrete and any deformations of the steel bar. If these disappear, the bar will pull out of the concrete and the tensile force, will drop to zero, causing the beam to fail. Bond stresses must present whenever the stress or force in a reinforcing bar changes from point to point along the length of the bar.

The bond in reinforced concrete beam can be lost due to corrosion or fatigue by cyclic load. The former one consumes the iron on the surface and let the section diameter decrease there by avoiding the contact between the reinforcement steel and the concrete. The later one occurred when there is high cyclic load and starts where there is a maximum moment in the structure

(beam). This loss of bond could propagate along the length of the beam. Obviously the effect is observable in flexural strength of RC beam. But its effect on the ultimate shear strength is not addressed to the required extent. And also test are being carried out on undamaged reinforced concrete beams, which mostly do not characterize what is present in reality.

Shear is an internal action in structures, due to the external transversal action, having the tendency of sliding (cracking) portion of a structure on the other (remaining) portion. In reinforced concrete members the vertical crack due to shear is resisted by the concrete alone, but its combined effect with flexure or pure shear could create a principal tensile stress inclined at some degree, in which the concrete is very weak, and lead the structure to failure in diagonal tension.

Shear in reinforced concrete beams is transferred by two load transfer mechanisms: beam action and arch action. If the shear flow across any horizontal plane between the reinforcement and the compression zone exists the shear is transferred by beam action. But if the shear flow cannot be transmitted, because the steel is unbonded, or if the transfer of shear flow is disrupted by an inclined crack extending from the load to the reactions, the shear is transferred by arch action rather than beam action, as shown in figure 1. In this member, the compression force C in the inclined strut and the tension force T in the reinforcement are constant over the length of the shear span. The extent of the beam action and arch action is also depends on the shear span to depth ratio (a/d ratio). In general, beam action is the governing load transfer mechanism in slender beams (a/d ratio greater than 2.5) whereas arch action is the dominant load transfer mechanism in deep beams (a/d ratio less than 2.5)

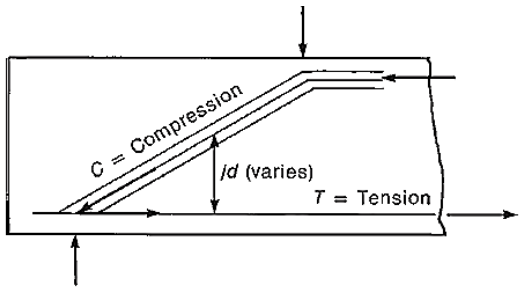

Figure 1-1 ***Arch action in a beam***

As it is clearly stated before the contact (bond) between reinforcing steel and concrete has its own effect in the shear behavior of reinforced concrete beam. Therefore, this thesis is

conducted to see the effect of loss of bond on shear behavior of short reinforced concrete beam, specifically determine the effect of loss of bond on the ultimate shear strength and to see the change in the crack pattern of reinforced concrete beam.

1.2 Significance of the research

Bond between the steel reinforcement and concrete is essential to ensure the composite interaction of the two materials. At very low stress, bond strength is mainly due to the chemical bond between the concrete and the steel bar but it becomes dependent on the mechanical interlock between the steel ribs and the concrete once slippage happens. There are many factors influencing the bond between the concrete and reinforcement steel, such as concrete strength, concrete composition and environments.

In most researches, conducted on loss of bond, the cause is considered to be corrosion in which the unbonding process occurs by the decrement of cross sectional area due to the consumed iron while the reinforcement steel is corroded. In this situation, since flexural strength is directly proportional to cross sectional area of the reinforcement steel, the reduction of steel area significantly affect the flexural capacity than shear. But in times, loss of bond may occur due to the application of cyclic load in which unbonding starts at the maximum point and propagate. Here the cross sectional area do not decrease and if the steel is anchored effectively reduction of flexural strength is less. But loss of bond could also affect the shear capacity. So this study is conducted to address the effect of loss of bond, without reduction in diameter of bar, on the ultimate shear strength of reinforced concrete beam.

1.3 Objective of the research

1.3.1 General objective

- To determine the effects of loss of bond on the behavior of ultimate shear strength of reinforced concrete beam.

1.3.2 Specific objective

- To unbond the reinforcement in different length and see their relative ultimate shear strength.
- To see how the crack pattern changes in each beam.
- To verify the experiment result using software.

1.4 Scope of the Work

This research program consists of experimental and analytical phases. The experimental phase comprises of testing four shear critical RC beams: one fully bonded control beams and three unbonded beams. The bottom reinforcing bars of the three beams are unbonded for 400mm, 800mm and 1200mm length. The beams will be tested monotonically under one-point loading. The analytical work includes the analysis of the control fully bonded beam and all the three unbonded beams using Vector 2. The results obtained from experiment are compared with the analysis results.

1.5 Organization of Thesis

The thesis is divided into five chapters as follows:

Chapter-1: This chapter describes the problem statement, significant of the research, objectives of the research program, scope of work and organization of the thesis.

Chapter-2: This chapter presents the literature review on the major influence on bond between concrete and reinforcement, factors that affect the bond strength of concrete and shear strength of RC beams corrosion in reinforced concrete and effect of corrosion on reinforced concrete beams.

Chapter-3: This chapter describes the experimental procedure including the fabrication of test specimens, instrumentation, test setup and procedure.

Chapter-4: This chapter presents the experimental results and discussion including monotonic test results and interpretation of the results.

Chapter-5: This chapter presents the main conclusions from this study and recommendation for future research.

CHAPTER 2 LITERATURE REVIEW

There are few things that must be examined in dealing with the effect of loss of bond on shear strength, first the process of unbonding must be clear, which includes how to unbond and the unbonded length. Then fully bonded specimen has to be examined to see what occurs there and the potential difference in the two scenarios. Lastly scientific papers will be presented related to the subject

2.1 Reinforcement-Concrete Bond

The bond between reinforcing steel and concrete is not fully understood, though a good working theory has been produced. Most of the main concepts are agreed upon, though some of the details are still being discussed. The reason for this is that the force transfer called bond is a complicated, multipart phenomenon. A useful method of describing the main forces is contained in Treece and Jirsa, they divide the main components into two main categories. The first is the bearing component on the lugs. This is what will cause splitting of the concrete. The second category is the friction component. This is both true friction and the effect of any secondary chemical bonding effects. A good summary of the major influences on bond is contained in Treece and Jirsa factors are, according to Nawy:

1. Adhesion between the concrete and the reinforcing elements.

2. Gripping effect resulting from the drying shrinkage of the surrounding concrete

3. Frictional resistance to sliding and interlock on the reinforcing elements subjected to tensile stress.

4. Effect of concrete quality and strength in tension and compression.

5. Mechanical anchorage effects of the ends of the bars through the development length, splicing, hooks and crossbars.

6. Diameter, shape and spacing of reinforcement as they affect crack development.

It is suggested that factors 2, 3 and 4 are most important. This list is not universally agreed upon, however, and current literature contains models for bond that focus more on the effects of bond rather than on absolute mechanisms. A typical mode1 is presented by Cairns and Jones

and Cairns and Bin Abdullah. They view bond as containing both a splitting and a non-splitting component. The splitting component varies with the amount of confinement that the bar experiences, while the non-splitting component is fixed. They do not explain what causes the non-splitting component, only that it is possibly similar to the cohesive effect in soils. Another variable that affects bond and has not been discussed so far is concrete confinement. Increasing the confinement around a bar increases its bond strength. This is true whether the confinement comes from transverse steel, e.g., stirrups, or from the stress field that exists in the concrete. This second situation can be explained best using an example. Where a beam intersects a column, the column load creates stresses that act perpendicular to the direction of the longitudinal beam steel. These stresses act to confine the steel and increase the bond strength. The influence of stress fields is not relied upon in design codes, though it is well accepted. This is because it is impossible to ensure that a stress field will always exist.

ACI 408, 2003 put the Bond-slip Mechanisms as it is between reinforcing bar and concrete comprises three distinct mechanisms: chemical adhesion, friction and mechanical interlock.

(i) Chemical adhesion: adhesion is the chemical bond created on the contact surface between the steel reinforcement and the surrounding concrete. This can be broken down at very low load, allowing slip between the reinforcing steel and the concrete.

(ii) Friction especially between the steel bar surface and concrete. The friction force plays a significant role between the concrete and the deformed bar (ribs).

(iii) Mechanical interlock: This shear bond becomes more significant with increasing relative displacement under composite mechanisms. The force transfer mechanism is primarily due to the mechanical interlocking between the ribs of steel and concrete. The mechanisms of chemical adhesion and friction are the most significant in the case of smooth bars (Figure 2.1). For deformed bars, the mechanical interlock of the steel bar ribs within the concrete is the principal mechanism which governs the bond strength-slip behaviour (Wang and Liu, 2003; Bamonte and Gambarova, 2007; Gambarova, 2012).

According to FIB (2000), the bond stress behaviour can be characterized by four stages, as shown in Figure 2.2 and described in the following paragraphs.

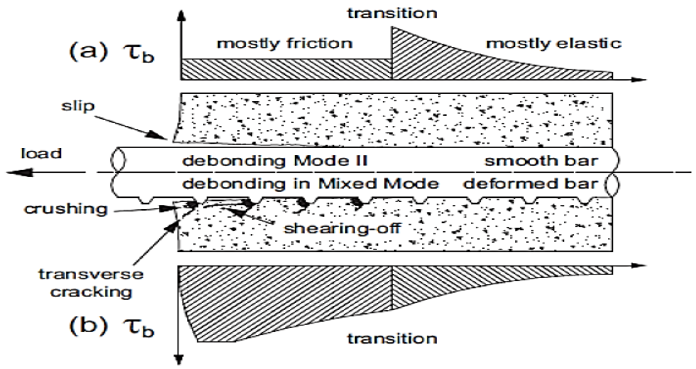

Figure 2-1 (a) ***Bond mechanisms in smooth bar; (b) Deformed bars (Bamonte and Gambarova, 2007)***

Stage I (uncracked), for low levels of bond stress, the main resistance mechanism is often chemical adhesion between the mortar matrix and the surface of the steel bar. At this stage, with low bond stresses, the resistance of the pulling forces for plain (smooth) steel bars relies only on chemical and physical adhesion. These bars have low bond performances suggesting that chemical and physical adhesion only play a minor role in the case of deformed bars and offer minimal resistance. As seen in Figure 2.2, the stress-slip relationship of this mechanism accounts for the low bond stress, $\tau < \tau 1$ where $\tau 1$ = (0.2 to 0.8) fct (FIB, 2000). Note that the relative displacement of the bar is always measured with reference to the undisturbed concrete and consists of two parts, the relative slip at the interface and shear deformations in the concrete

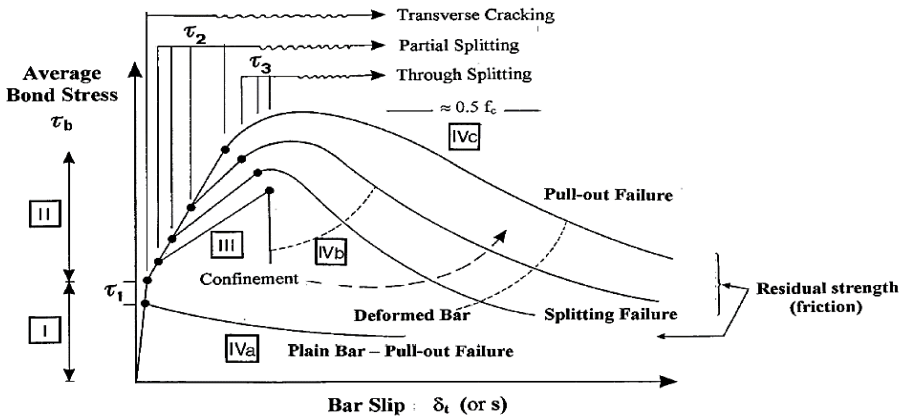

Figure 2-2 ***Bond stress-slip (FIB, 2000)***

Stage II (first cracking) is when an increase in the bond stress results in the loss of the chemical and physical adhesion. Large bearing stresses under the lugs of deformed bar are induced by the interaction between the ribs and concrete. Transverse micro cracks result at the tips of the

ribs and allow the bar to slip, however, the wedging of the lugs remains small enough not to induce concrete splitting (FIB, 2000).

Stage III occurs when the concrete material directly in front of the ribs crushes as the bond stress values develop to around (1-3) *f*ct (FIB, 2000), forming a crushed concrete wedge in front of the lugs of the bar. The slip of the bar is mainly attributed to the crushing of the concrete material. It should be noted that the wedge has a smaller angle than that of the face of the ribs, enhancing the wedge action of the deformed bar on the concrete which is enhanced by the crushed concrete stuck to the front of the lugs (Paulay and Park, 1975). As a consequence, the layer of concrete surrounding the bar exerts a confinement condition on the bar owing to the reaction of hoop stresses, which is upheld until the wedging forces reach the level of hoop stress and develop longitudinal cracks, initialising splitting failure. The bond stress increases until a split reaches the outer surface which is known as through splitting (**τ3**) as shown in Figure the magnitude of **τ3** is dependent on the degree of confinement.

Stage IV initialization depends on the level of transverse reinforcement. Following the attainment of the **τ3** bond stress value, the longitudinal splitting cracks break through the whole concrete cover and result in failure. Shear links and stirrups surrounding the bar may still contribute to the bond efficiency after this point and maintain the strength despite large slip values. As shown in Figure the curve is representative of a bar with light to medium transverse reinforcement.

2.2 Factors affecting on the bond strength of concrete

Bond strength between the steel reinforcement and concrete is affected by many factors. Important amongst these factors are the steel reinforcement properties, concrete properties and other environment factors (i.e. corrosion and temperature). These factors which influence the bond strength steel/concrete interface are discussed in detail in the following sections.

- Effect of bar profile

Steel reinforcement geometry largely contributes to bond strength. It has been recognized that deformed bars have better bond properties than smooth bars. The reason is that deformed bars benefit from the mechanical anchorage supplied by the concrete keys between the ribs. A number of investigations were carried out to determine the influence of the rib height on bond behavior. The results showed that for unconfined bars, the relative rib area (*R*r) (defined as the

projected rib area normal to the bar axis divided by the nominal bar perimeter multiplied by the center to center rib spacing) has no influence on bond strength. For confined bars, however, the bond strength increases by increasing the relative rib area (ACI 408 2003). In this way, the bond strength of reinforcing bar is a function of relative rib area. In general, increasing the relative rib area of steel bar, increases the bond strength (Cairns and Abdullah, 1995; Darwin and Graham, 1993; El-Hacha et al., 2006). Recently, Chan (2012) investigated the effect of different grades of deformed bar types with different rib patterns and relative rib area (*Rr*) on bond strength. It was observed that the specimens with steel bars which had the higher *Rr* exhibited higher bond stress.

- Effect of bar diameter

The steel bar size is one of the most important factors affecting the bond stress between steel reinforcement and the surrounding concrete. The ribbed bar influences the bond strength, while larger bar diameters develop lower bond strength compared to smaller bar diameters. This effect is acknowledged in ACI 408 (2003) by suggesting a steel bar size factor in its development length formula. Moreover, the influence of reinforcing bar diameter on the bond strength has been investigated by several researchers. Ichinose etal. (2004) have provided experimental evidence that the influence of the bar size on the bond strength depends on the level of confinement. In their tests, the bond strength was found to decrease with increasing bar size for specimens with low levels of confinement and splitting failures, but this effect was negligible for specimens with high levels of confinement and pull-out failures. This was somewhat supported by Turk and Yildirim (2003) who reported that the diameter of the steel bar had a very important effect on the bond strength. Other researchers, such as De Larrard et al. (1993) reported that the bond strength of a 10mm diameter reinforcing bar was higher than that of large diameter steel reinforcement suggesting that the bond strength decreased with increasing diameter of steel reinforcement.

- Effect of compressive and tensile strength of concrete

The bond strength mechanism is actually dependent on the stress transfer from the steel reinforcement to the concrete with compression and shear interaction forces. Therefore, the bond behaviour is dependent on both the compressive and the tensile strength of concrete. When considering splitting and pull-out modes of bond failure, the tensile strength *f*ct of concrete is a more important parameter than the compressive strength because splitting is approximately proportional to (*fc*') 1/2, where *fc*' is the compressive strength of concrete and

the bond strength traditionally has been indicated as (fc')1/2. However, regression analysis on different experimental results showed that a superior correlation exists between bond strength and (fc')1/4 for bond failure (ACI 408 2003). Arel and Yazici (2012) investigated the effect of different compressive strength and tensile strength of concrete on the bond strength between steel and concrete. The concrete strength ranged between 13.46 to 75.40 N/mm2. They found that the bond strength increased with an increase in both the compressive strength and tensile strength of concrete. Kankam (2003) studied the influence of concrete grade on the bond strength by using two different concrete grades (53 N/mm2 and 31 N/mm2). It was found that the higher concrete strength specimen had greater bond stress than the specimen with lower concrete strength. In another study, Valcuende and Parra (2009) studied the bond strength of steel reinforcement embedded in self-compacting concrete (SCC) and vibrated concrete (VC). This can be explained by the differences between the two types of concretes which vary with the compressive strength. In addition, this may possible be explained by SCC having greater fill capacity, which enables them to cover the reinforcements completely without the need for vibrators and its smaller amount of bleeding also reduce the occurrence of voids between the steel and concrete but in VC the process depends on the vibration treatment being correct.

- Effect of concrete cover

The concrete cover is the distance between the reinforcing bar surface and the exterior face of the concrete element. It is another important parameter which governs bond stress failure. The increase of cover thickness can increase the bond stress at failure as a result of increasing the confinement on the steel bar prior to failure. Some authors have studied the effect of concrete cover on bond strength; they reported that the bond strength was increased with increasing the depths of concrete cover (Tepfers 1979 and Chana, 1990). Recently, Yalcier et al. (2012) studied the influence of concrete cover thickness of three different depths (i.e. 15mm, 30mm and 45mm) on bond strength. They reported that the bond strength was significantly increased when the concrete cover depth increased and the bond specimens were failed by pull-out failure.

- Other factors

There are other factors that influence the bond strength between reinforcing bar and concrete, including environmental effects such as steel bar rusting. The effect of the corrosion of steel reinforcement on structural behavior is considered a major issue today, as demonstrated by many experimental studies (Almusallam et al., 1996; Lee et al., 2002; Lundgren, 2002; Fang

et al., 2004 and Dahou et al., 2009). This factor will be explained in further detail in the following section. In addition, high/low temperatures affect bond strength as reported by Royles and Morley (1983) Van der Veen (1992). Bingöl and Gül (2009) reported that the residual bond strength increased when temperature ranged from 50˚C to 150˚C due to the increase in the residual compressive strength. After that, the residual bond strength was decreased as temperature reached 150˚C. Moreover, Haddad et al. (2008) studied the influence of elevated temperature on bond strength of steel bar embedded in concrete. They found that the residual bond strength decreased slightly as the exposure temperature was raised to 350 ˚C due to the increase intensity and cracks with temperature leading to a reduction in concrete confinement of the steel reinforcement.

The unbonding process will avoid the major influences which are mentioned above. To prevent the direct contact between the reinforcing steel and concrete rigid plastic tube will be used, in which the reinforcing steel is going to be inserted. Quarter, half and full length of the beam will be unbonded separately and each specimen test shall be compared to the control beam.

Previous researches has been reviewed with regard to the subject and one of them is *Shear behavior of RC beams with corrosion damaged partial length* published by *Xiao-Hui Wang • Bing Li • Xiang-Hua Gao* in 9 September 2011, this paper presents experimental study on shear behavior of reinforced concrete (RC) beams with corrosion damaged partial length in one shear span.

In order to discover how mechanical behavior and load capacity of the RC beam were influenced by the corrosion damaged partial length, 14 RC beams including two noncorroded RC beams, four RC beams with partially unbonded length and eight RC beams with partially corroded length were designed. The different shear span-to-effective depth ratios, the different designed partial lengths located in one shear span and the different corrosion levels within the designed partial lengths were the main considered parameters.

In the experimental detail the all specimens were rectangular cross section of b × h = 150 × 180 mm, with the overall length of the beam 1800 mm and a 1200 mm distance between supports. All beams were designed to fail in shear by providing three 16 mm diameter deformed bars as longitudinal flexural reinforcements to exclude premature flexural failure. Two top 6 mm-diameter plain bars were used to serve as stirrup-holders in the compression zone. 6 mm-diameter plain bars were also served as the shear reinforcement. Two different shear span-to-

effective depth ratios 2.0 and 3.0 were chosen. With a material property of concrete made in laboratory with target strength of 30 Mpa and water-to-cement ratio of 0.55. Normal Portland cement and coarse aggregate with maximum aggregate size of 20 mm were used in the concrete mixture. The concrete mixture proportion by weight was as follows: cement: water: sand: gravel = 1:0.55:1.56:2.90. The 16 mm diameter deformed bar had average yield and ultimate strengths of 339.4 and 550.8 Mpa, respectively; while the 6 mm diameter plain bar had average yield strength of 441.5 Mpa.

For the test specimens with partially unbonded length, the cracking patterns were fundamentally different from that of the control RC test specimens. Due to the complete elimination of bond within the partial length, a drastic change in failure mode was also observed. Unlike the control RC beam, at a very low loading, only 40–80 le (8.9–17.9 kN), the first vertical crack was observed at the interior edge of the partially unbonded length. With the increase of the loading, this crack quickly propagated, appearing at the top and bottom surface of the beam. Later, the flexural crack was observed near the mid-span of the specimen. Due to the absence of the bond-induced shear stress within unbonded length, no inclined cracks were observed in the shear span with unbonded length. The inclined cracks only appeared in the other shear span, propagating further in both directions.

For beams B2.0-200-0 (a beam with shear span-to-effective depth ratio 2.0, having 200 mm target partial length in one shear span and complete loss of bond within the target partial length). and B2.0-300-0(a beam with shear span-to-effective depth ratio 2.0, having 300 mm target partial length in one shear span and complete loss of bond within the target partial length), the average tensile strains at the mid-span firstly reached the yielding strain of the noncorroded longitudinal reinforcing bar, with a slight increase of the loading, the tensile steel within the partial length yielded. Then, the stirrup yielded and wider shear cracks developed with further increase of the loading, resulting in the stirrup fracture.

While for beam B3.0-300-0(a beam with shear span-to-effective depth ratio 3.0, having 300 mm target partial length in one shear span and complete loss of bond within the target partial length) and B3.0-450-0(a beam with shear span-to-effective depth ratio 3.0, having 450 mm target partial length in one shear span and complete loss of bond within the target partial length), the average tensile strains in partial length firstly reached the yielding strain of the noncorroded longitudinal reinforcing bar at the center, with a slight increase of the loading, the average tensile strains longitudinal reinforcement at the center reached the yielding strain.

Then, for beam B3.0-300- 0(a beam with shear span-to-effective depth ratio 3.0, having 300 mm target partial length in one shear span and complete loss of bond within the target partial length), the average strains of longitudinal reinforcement at center increased fast than those of longitudinal reinforcement in the partial length, resulting in typical flexural failure—wider flexural cracks and crushing of concrete in the constant moment zone. For beam B3.0-450-0(a beam with shear span-to-effective depth ratio 3.0, having 450 mm target partial length in one shear span and complete loss of bond within the target partial length), although the average tensile strains also quickly increased with further increase of the loading, the yielding of the stirrups and wider developed shear cracks resulted in the beams failing in the stirrup fracture.

Other reinforced concrete books, based on simple cracked section analysis, has also showed the relation, as presented below, between bond and shear. Bond stresses must be present whenever the stress or force in a reinforcing bar changes from point to point along the length of the bar. This is illustrated by the free-body diagram in Figure 2.3. If *f*s2 is greater than *f*s1, bond stresses, μ, must act on the surface of the bar to maintain equilibrium. Summing forces parallel to the bar, one finds that the average bond stress, μ*ave* is

$$(f_{s2} - f_{s1})\frac{\pi d_b^2}{4} = \mu_{\text{avg}}(\pi d_b)\ell$$

and taking *f*s2-*f*s1=Δ*f* gives

$$\mu_{\text{avg}} = \frac{\Delta f_s d_b}{4\ell}$$

If *l* is taken as a very short length, *dx*, this equation can be written as

$$\frac{df_s}{dx} = \frac{4\mu}{d_b}$$

Where **m** is the *true bond stress* acting in the length *dx*

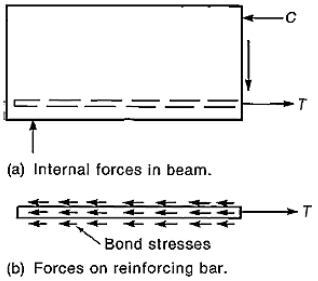

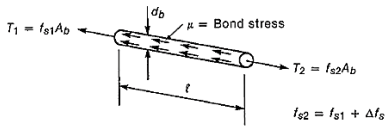

Figure 2-3 ***Relationship between change in bar stress and average bond stress***

Average Bond Stress in a Beam

In a beam, the force in the steel at a crack can be expressed as

$$T = \frac{M}{jd}$$

Where *jd* is the internal lever arm and *M* is the moment acting at the section. If we consider a length of beam between two cracks, as shown in Figure below, the moments acting at the two cracks are M_1 and M_2 if the beam is reinforced with one bar of diameter d_b the forces on the bar are as shown in Figure 2.4c. Summing horizontal forces gives

$$\Delta T = (\pi d_b)\mu_{\text{avg}}\,\Delta x$$

where d_b is the diameter of the bar, or

$$\frac{\Delta T}{\Delta x} = (\pi d_b)\mu_{\text{avg}}$$

But

$$\Delta T = \frac{\Delta M}{jd}$$

Giving

$$\frac{\Delta M}{\Delta x} = (\pi d_b)\mu_{\text{avg}}\,jd$$

From the free-body diagram in Figure d, we can see that $\Delta M = V\Delta x$ or $\Delta M/\Delta x = V$. Therefore,

$$\mu_{\text{avg}} = \frac{V}{(\pi d_b)jd}$$

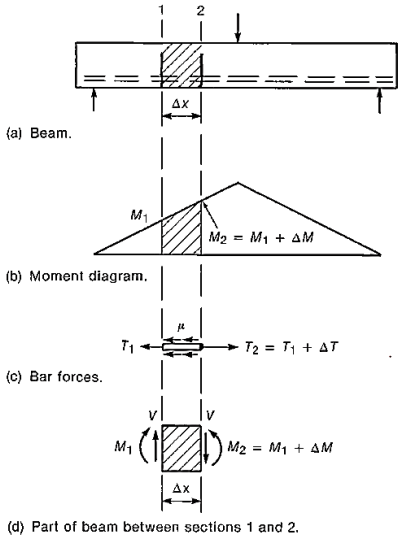

Figure 2-4 ***Average flexural bond stress***

If there is more than one bar, the bar perimeter ($\prod d_b$) is replaced with the sum of the perimeters, $\sum_0$, giving

$$\mu_{avg} = \frac{V}{\sum ojd}$$

The above two equations give the *average bond stress* between two cracks in a beam. As shown later, the actual bond stresses vary from point to point between the cracks.

"*Influence of Longitudinal Bar Corrosion on Shear Behavior of RC Beams"* has also been studied by *Xin Xue and Hiroshi Seki.* In this research experimental investigations were conducted to investigate the shear behavior of RC beams with corroded longitudinal bars, in which parameters such as corrosion level and shear-span-to-effective-depth-ratio were taken into consideration. Analytical investigations were also performed to evaluate the load-carrying mechanism of these specimens.

The geometry and reinforcement arrangement of the specimens are shown in Figure below. The specimens had the same cross section of 120 mm in width, 240 mm in overall height, and 220 mm in effective depth. The specimens had three types of length to take into consideration the influence of shear span. Ultra-high strength steel bars D19 (Specific: USD685A, *fy* = 706 N/mm2) were used as longitudinal bars to acquire strong flexural strength. The steel ratio was designed as 1.9%, which is similar to that of conventional beams. To prevent the specimens from anchorage failure, the longitudinal bars were fixed to the steel plates placed outside the specimens using nuts.

The experimental parameters were shear-span-to effective- depth-ratio (*a/d*) and corrosion level of the longitudinal bars. Apart from the specimens with an a/d of 2.6, which was thought to be sensitive to failure mode, specimens with four other different a/d (1.5 ~ 4.0) were also fabricated. The specimens can be grouped into several series with the same a/d, each series containing one sound specimen and two or three corroded specimens with different corrosion levels. For example, the B(2.6)-m series represented a group of specimens with an a/d of 2.6, and involved one sound specimen B(2.6)-m and three corroded specimens B(2.6)-m1~m3. Since severe corrosion would result in anchorage failure due to the dramatic decrease in bond strength, which is beyond the scope of this paper, the maximum percent average mass loss (to be specified later) used to describe the corrosion level, was set as 20%.

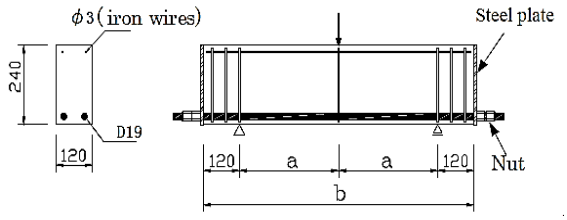

Figure 2-5 ***Specimen detail***

Load test

The specimens were subjected to load tests under simply supported conditions, as shown in Figure 2.5. The load was applied to the middle span with a displacement increment of 0.2mm/minute. Application of the load was monitored using a load cell, and the deflection at the mid-span was measured using displacement transducers placed under the specimens.

Experimental results

The experimental results are summarized in Table, in which the compression strength of concrete *fc'*, percent average mass loss *C*, and the shear behavior such as failure load *Ptest* and failure mode were specified. The specimens were divided into three groups to describe their experimental results respectively:

Specimens with short shear span a/d=1.5

Specimens with moderate shear span a/d=2.0, 2.6

Specimens with long shear span a/d=3.5, 4.0

Table 2.1 ***Experimental result***

Specimens	f'_c (N/mm2)	C (%)	P_{test} (kN)	Failure mode
B(1.5)-m	36.0	0.0	199.4	Splitting
B(1.5)-m1	35.1	2.7	200.6	Splitting
B(1.5)-m2	36.8	6.7	195.9	
B(1.5)-m3	36.8	10.4	200.8	
B(2.0)-m	43.0	0.0	123.8	Shear compress
B(2.0)-m1	46.4	3.8	183.6	
B(2.0)-m2	44.7	15.0	191.6	Support flexure
B(2.6)-m	33.1	0.0	86.4	Diagonal tension
B(2.6)-m1	35.1	7.0	101.4	Shear compress
B(2.6)-m2	36.2	13.9	124.9	
B(2.6)-m3	36.2	17.0	111.0	Support flexure
B(3.5)-m	43.0	0.0	79.7	Diagonal tension
B(3.5)-m1	45.8	5.4	78.8	Bond splitting
B(3.5)-m2	44.7	7.3	61.9	
B(4.0)-m	35.2	0.0	66.8	Diagonal tension
B(4.0)-m1	34.7	3.7	60.3	Bond compress
B(4.0)-m2	33.7	4.9	53.7	Bond splitting

Load test results

Specimens with short shear span (a/d=1.5)

Experimental results of the B (1.5)-m series are summarized in Figure 2.6. Regarding load-displacement relationship, compared to the sound specimen B (1.5)-m, the corroded specimens exhibited a slight decrease in post-diagonal-crack stiffness, but no change in shear capacity.

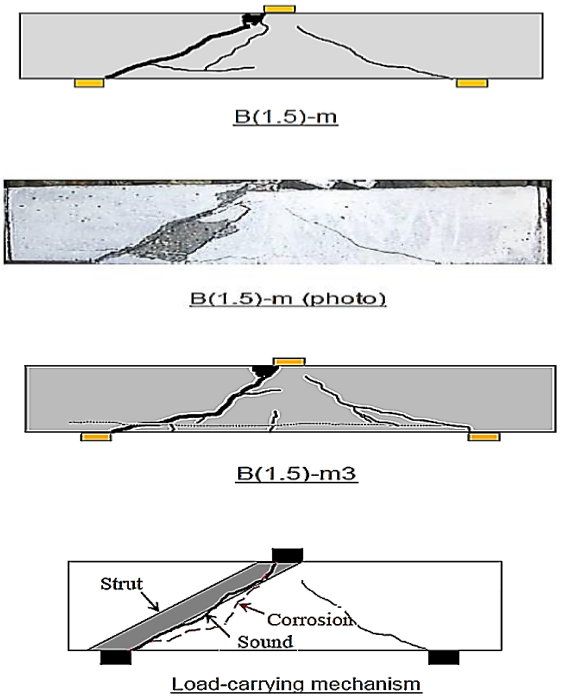

Figure 2-6 ***Load test results of B (1.5)-m series.***

Specimens with moderate shear span (a/d=2.0, 2.6)

Two main conventional failure modes were observed during the load tests. One is diagonal tension failure caused by a type of concrete splitting along one critical diagonal crack, and another is shear compression failure due to the crush of concrete near the loading point. Figure 2.7shows the load test results of the B(2.0)-m series. Both the sound specimen B(2.0)-m and the corroded specimen B(2.0)-m1 failed in shear compression, whereas B(2.0)-m2, whose longitudinal bars were severely corroded, failed in a splitting mode.

B(2.0)-m

B(2.0)-m1

Specimens with long shear span (a/d=3.5, 4.0)

Because B (3.5)-m series share similarities with B (4.0)-m series in the shear behavior, only the experimental results of the B(4.0)-m series are discussed here. The results are shown in Figure 2.8. Compared to the sound specimen, the diagonal cracks in corroded specimens shifted slightly toward the loading point.

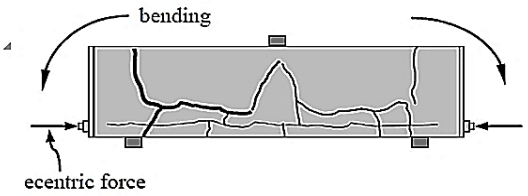

B(2.0)-m2

(b) Crack pattern at failure

Figure 2-7 ***Load test results (a/d=2.0).***

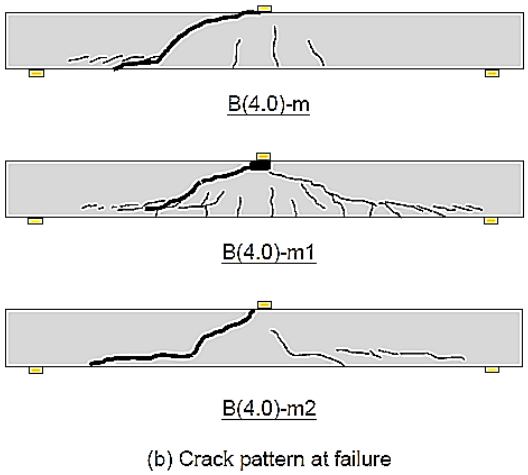

Figure 2-8 ***Load test results (a/d=4.0).***

2.3 Analytical investigation

Outline of analysis

Analytical model

A two-dimensional nonlinear analysis was conducted in this paper. The analytical model is shown in Figure 2.9. Because of the symmetry, the left side of the specimen was chosen for analysis and the middle cross-sectional plan was confined in the x direction. To prevent areas near the loading point and support from local failure, elastic elements with strong stiffness was adopted in the model. The concrete matrixes and the longitudinal bars were modeled using iso-parametric elements and truss elements respectively, and interface elements were introduced in between to model the bond effects. Taking into consideration of the full anchorage of longitudinal bars in the experimental specimens, the longitudinal bar elements outside the support were modeled as perfect bond to the concrete elements. The mesh size was determined in accordance with the maximum coarse aggregate. Modified Newton-Raphson method was used in iteration procedure and convergence is judged by energy norm. A smeared crack model was adopted to simulate the crack occurring in the concrete.

Constitutive law

The stress-strain behavior of concrete is shown in Figure 2.10(a). In the compression zone, the stress increases following a parabolic curve before it reaches compression strength, and then decreases linearly as strain progresses. In the tension zone, the stress increases linearly before it reaches tension strength, and then decreases following a tension softening model proposed

by Hordijk (Hordijk 1991). To reduce the influence of mesh division, the parameters of fracture energy *Gf* and *Gc* were introduced in the tension and compression zones respectively to decide ultimate strain. For the longitudinal bars, the yield condition of Von Mises without consideration of strain hardening was adopted. The stress-strain relationship is shown in Figure 2.10(b). Regarding the bond behavior between the longitudinal bars and the concrete, a τ-s relationship proposed by Dörr (1980) was adopted, which shows a limit in shear strength if the slip is larger than a certain value (see Figure 2.10(c)).

$$\tau = \begin{cases} c\left(5\left(\frac{s}{s_0}\right) \;\; 4.5\left(\frac{s}{s_0}\right)^2 + 1.4\left(\frac{s}{s_0}\right)^3\right) & \text{if } 0 \le s \le s_0 \\ 1.9c & \text{if } s \ge s_0 \end{cases}$$

$$where \;\; c = f_t \;\; , \;\; s_0 = 0.06mm$$

where *ft* is tensile strength of concrete. In the corroded specimens, the influence of longitudinal bar corrosion on bar mechanical properties and the bond behavior between bars and concrete was modeled. The young's modulus and the yield strength of corroded longitudinal bars were reduced using the following equation (JSCE 2006), given that there was no change in the cross-section (see Figure 2.10(b)).

$$f_y / f_{yo} = 1.00 - 2.17 \times C/100$$

$$E_s / E_{so} = 1.00 - 1.13 \times C/100$$

Where *fy* and *Es* are the yield strength and the young's

$$\tau_b / \tau_{bo} = \exp(-0.0607 \times C)$$

Where τ_b is the bond stress of corroded longitudinal bars, τ_{b0} is the bond stress of sound longitudinal bars.

Shear behavior after cracking

In concrete beam members, even after diagonal cracks occur, the shear stress can also be transferred cross the cracks due to the aggregate interlock action along the crack surface. However, the shear stiffness of cracked concrete should be reduced gradually as the crack opening progresses and shear strain γ increases, which is also called shear softening. For this reason, a shear retention factor β was introduced to take into consideration this shear stiffness reduction, and the shear softening was modeled using a bilinear β-γ relationship shown in Fig. 2.10(d). Because the shear softening is supposed to be influenced by the shear span (Tadokoro

et al. 2003), a parametric study was conducted and based on its results different appropriate β-γ relationships were decided for each series of specimens.

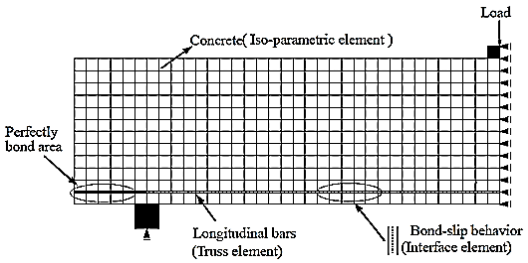

Figure 2-9 ***Analytic model***

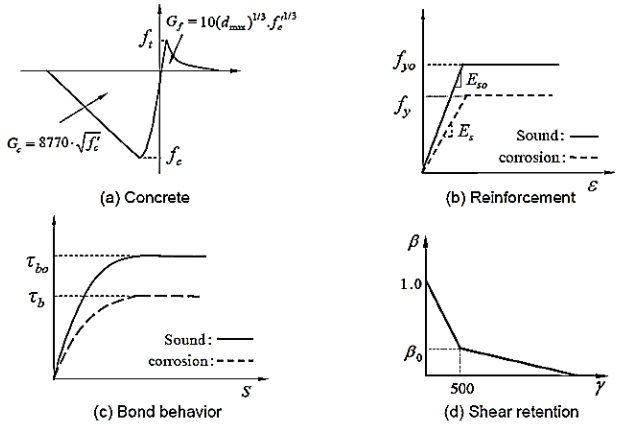

Figure 2-10 ***Constitutive law***

Analytical output

(1) B (1.5)-m series

The analytical output of the B (1.5)-m series is shown in Figure 2.11 Except for the post-peak behavior, the analytical output agrees with the experimental results (see Figure 2.11(a)). Judged from the brittle failure mode observed during the load test, it should be noted that the post-peak behavior described by the analytical output seemed to be more reasonable. The irrational behavior of the experiment is thought to be caused by the load-applying method. Regarding the influence of longitudinal bar corrosion, there is little change in the load-displacement relationship between sound and corroded specimens (see Figure 2.11(b)), which coincides with that of experimental results. As for crack pattern at failure, the analytical output agrees with

experimental results in sound specimens, but for corroded specimens, it cannot completely reproduce the crack pattern observed in the experiment. Those of sound longitudinal bars. Regarding the bond behavior of corroded longitudinal bars, the whole bond stress was reduced using the following equation (JSCE 2006). However, the analytical output revealed that all specimens failed in the same brittle style: after a diagonal crack initiated, it propagated rapidly toward the loading point and the support as applying load increased, and consequently it penetrated the cross section and caused an abrupt decrease in load-carrying capacity.

(2) B (2.6)-m series

Figure 2.12 shows the analytical output of the B (2.6)-m series. Except for the post-peak behavior, the analytical output coincides with the experimental results (see Figure 2.12(a)). Regarding the load-displacement relationship, the corroded specimens exhibited a clear decrease in post-crack stiffness, and a significant increase in shear capacity (see Figure 2.12(b)), which coincides with the experimental results. The shift of the critical diagonal crack toward the loading point in corroded specimens was also completely reproduced by the analytical output (see Figure 2.12 (c)). As described in the experimental results, this is due to the buildup of tie-arch mechanism. The distribution of stress along the longitudinal bar at failure is shown in Figure 2.12(d). In the sound specimen, the stress decreased linearly from mid span to the support, which implies that the tensile stress of the longitudinal bars was transferred to the concrete due to the perfect bond effect. In corroded specimens, however, the stress along the bars exhibited hardly any change within the shear span, which implies that the tensile stress of longitudinal bars could not be transferred to concrete but to the anchorage due to the deterioration of bond strength. As a result, beam mechanism weakened and the tie-arch mechanism built up. Figure 2.12(d) provides additional evidence towards the conclusion drawn from the experimental results that, to state here again, the corrosion of longitudinal bars may cause a transition in the load-carrying mechanism.

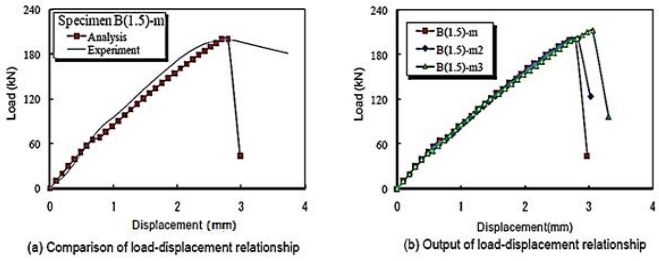

(a) Comparison of load-displacement relationship
(b) Output of load-displacement relationship

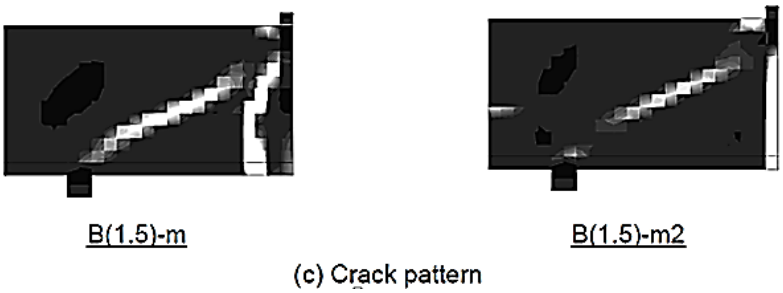

(c) Crack pattern

Figure 2-11 Analytical output of B (15)-m series

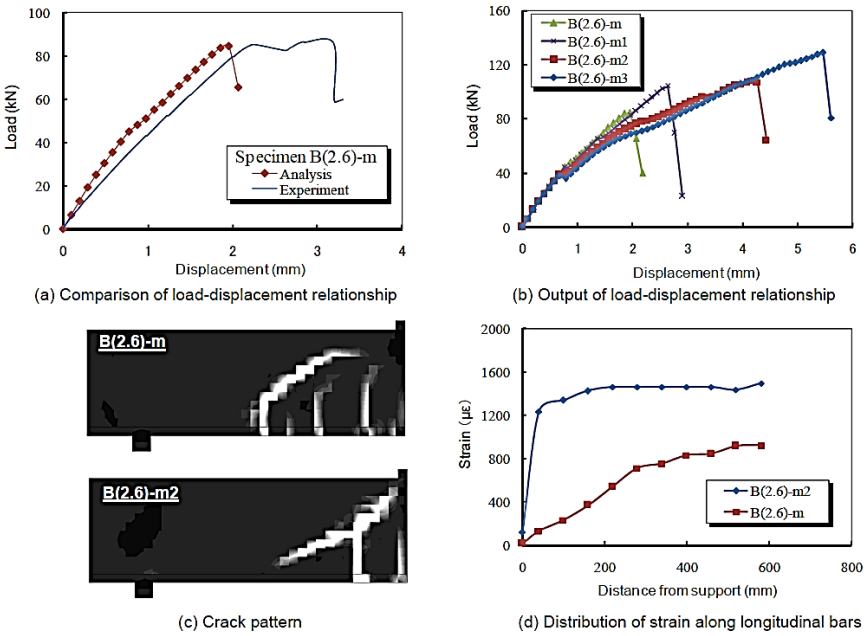

(a) Comparison of load-displacement relationship

(b) Output of load-displacement relationship

(c) Crack pattern

(d) Distribution of strain along longitudinal bars

Figure 2-12 *Analytical output of B (2.6)-m series*

CHAPTER 3 EXPERIMENTAL PROCEDUREE

The experimental procedure is presented to show the process involved to investigate the effect of unbonding of the longitudinal reinforcement on the shear behavior of reinforced concrete (RC) beams. The details of the experimental program including the design of the test specimens, instrumentation, and test setup procedure are presented in the following sections.

3.1 Materials

3.1.1 The Concrete

Concrete Mix Design

Data Required for Concrete Mix Design

Characteristic compressive strength required at 28 days grade designation M-25

Nominal maximum size of aggregate

Economical

Consistent with dimension of the structure

< 1/5 narrowest dimension between side of forms <30mm

< ¾ clear spacing between individual reinforcing bars

Maximum nominal aggregate size - 20mm

Shape of CA — Angular

Degree of workability required at site — 50-75 mm (slump)

Type of cement: OPC conforming IS: 455

Test data of material

Specific gravity of cement — 3.15

Specific gravity of FA — 2.64

Specific gravity of CA — 2.84

Aggregate are assumed to be in saturated surface dry condition.

Having the given data the ratio is: ***Cement: F.A: C.A=1:1.9:3***

Table 3.1 ***mix ratio***

w/c	0.5
25mm Aggregate	1108.88 kg/m^3
Sand	710.67 kg/m^3
Water	191.08 kg/m^3
Portland Cement	382.16 kg/m^3
Slump	55mm

With this proportion the third day compressive strength for three cube test is 13.22 MPa, 14.47 MPa, and 15.98 MPa. The average of these is 14.56 MPa which is 58.24% of the 28th day strength, so it is accepted.

3.1.2 The Reinforcing steel

The main reinforcing steel used was ϕ24 bar with a nominal strength of 500MPa obtained commercially, and its actual yield strength and ultimate strength obtained from test was 582MPa and 666MPa respectively. The top reinforcement, provided for holding the stirrup and increase compressive flexural strength, was ϕ10 bar with yield strength of 555.41MPa and ultimate strength of 694.27MPa, and since the specimens are expected to fail in shear the minimum steel diameter, ϕ6 bar, has been used for the stirrup with yield strength of 548.5MPa and ultimate strength of 591.8MPa.

3.2 Structural testing

3.2.1 Specimens' details

One standard structural specimen was used for al1 the structural tests. It was selected for the size such that it would fail in shear. Rectangular cross section specimens were used with b=200mm and depth, h =300mm, the overall length of the beam is 1800 mm and a 1200 mm distance between supports. All four beams are provided with 24mm diameter deformed bar as longitudinal flexural reinforcement to avoid premature flexural failure and in compression zone two 10mm diameter deformed bars were used to hold stirrups. 6 mm-diameter plain bars were also used to serve as the shear reinforcement and these stirrups spaced uniformly at 200 mm along the length of the beam. The bottom reinforcements are inserted in pipes in different length to create loss of bond. Three of the beams were casted with 1/3(400mm), 2/3(800mm) and full length (1200mm) unbonded of the total length between the supports and one beam were casted fully bonded, which is a control beam. The beam details are shown in the figure a & b.

Table 3.2 ***Details of test specimen***

Specimen	Target fc' (MPa)	Longitudinal Reinforcement			Shear Reinforcement fy 548.5 MPa
		Amount of reinforcement	Steel ratio(ρ)	Unbonded partial length(cm)	
CB:PL_0	25.6	3ϕ24_fy 582MPa	0.022619	0	6mm@200mm c/c
PL_40	25.6	3ϕ24_fy 582MPa	0.022619	40	6mm@200mm c/c
PL_80	25.6	3ϕ24_fy 582MPa	0.022619	80	6mm@200mm c/c
PL_120	25.6	3ϕ24_fy 582MPa	0.022619	120	6mm@200mm c/c

The designation PL stands for the unbonded partial length of steel reinforcement, so PL_0 means a specimen having 0cm unbonded reinforcement steel (fully bonded) and PL_120 is a specimen with 120cm unbonded reinforcement steel (unbonded between support to support). Since the beams are unbonded, the reinforcement are susceptible to slip. In order to avoid this critical concern the minimum anchorage length of the tensile reinforcing bar for the deformed steel is provided so that the specimens would fail in the predetermined shear failure rather than unwanted anchorage failure.

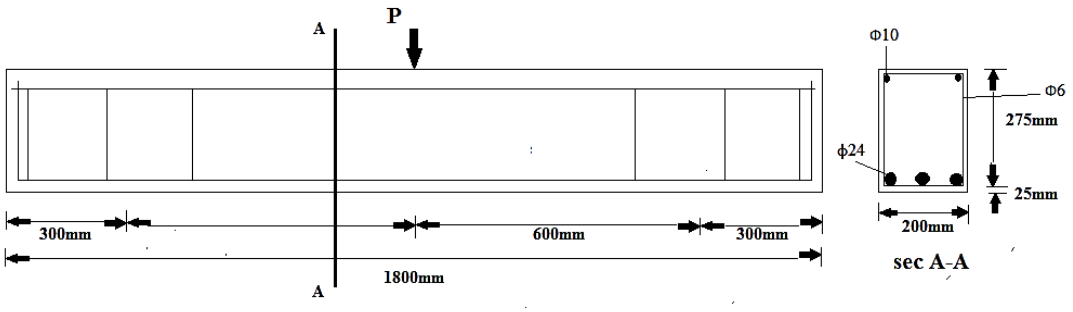

a)

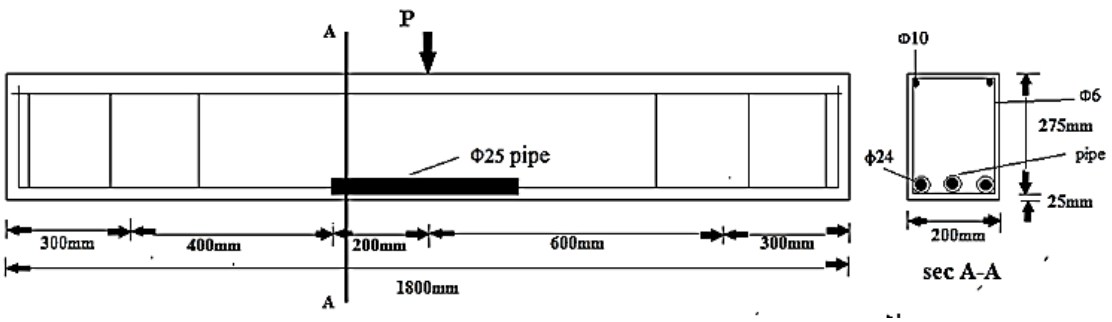

b)

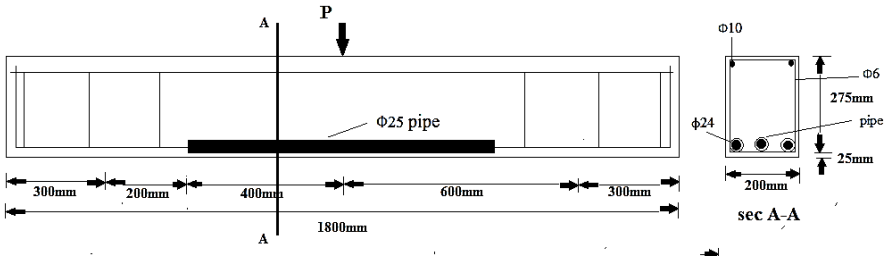

c)

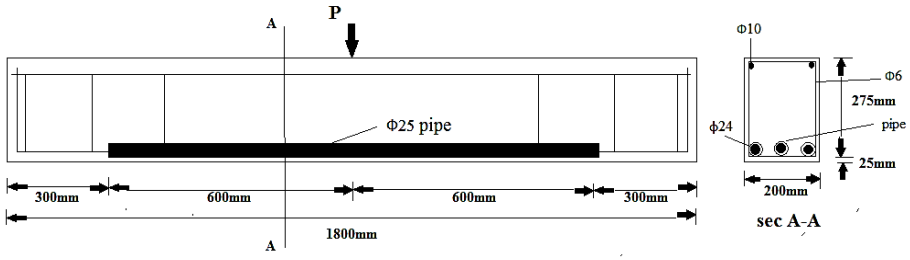

d)

Figure 3-1 ***Test specimen detail a) control beam_PL0 b) Partial 40mm unbonded length_PL40 c)Partial 80mm unbonded length_PL80 d) Partial 120mm unbonded length_PL120***

a)

b)

Figure 3-2 ***a) A tied rebar beam cage for 120mm & 40mm unbonded length beam b) A tied rebar beam cage for 80mm partial length & control beam***

The concrete mixed by a mixer in two batches and the first batch used to cast beams with 40mm & 80mm partially unbonded length. Beam with 120mm partially unbonded length & control beam, which is fully bonded, casted using the second batch. The slump, for both mixes, were within the assumed limit in the mix ratio. 51mm & 45mm for the first and second mix (batch) respectively. A total of six concrete cubes were casted from the same batch

Figure 3-3 ***slump for the mix***

The beams were cast in formwork that consisted of a wooden base and wooden sides. The formwork was lubricated before casting the concrete for ease of stripping the beams. The reinforcement cages were 25mm away from the base and each side of the formwork by inserting 25mm depth precast mortar in order to provide cover to the main longitudinal reinforcement.

3.3 Loading test

All beams were tested by one point loading test. But before the test carried out, each beam was placed over supports, leveled and centered under the point load system. Once the beam was leveled and centered, LVDT's were mounted at mid-span under the point load. One LVDT was used to measure the downward deflection relative to the support point. This was done by connecting a straight wood to the beams at the support point and hanging the transducer on it at 0.6m distance from each support, and then, the instrumentation (LVDT's and Load cell) was connected to data logger. The data logger started gathering data just before the application of load. The beam was loaded manually by hydraulic jack until failure of beam. During the test, the initiation and progression of cracks was monitored in order to understand the behavior of the tested beams.

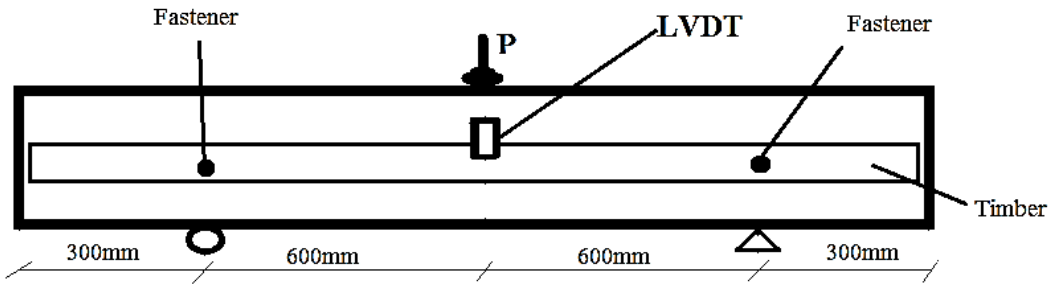

Figure 3-4 ***Testing Set-Up Schematic***

3.4 Material test

Three concrete cubes were taken from each batch to test the 28th day compressive strength of the beam and these cubes are cured by pouring water with the beams for 28 days to simulate the exact condition of the beam

Figure 3-5 ***sample cube and specimen***

After 28 days the compressive strength of each cube were tested and there appears some discrepancy with the first mix ratio estimation, but the difference between the two mixes (batches) is insignificant. And since the main concern of the research is not concrete strength, the result has been adopted.

CHAPTER 4 EXPERIMENTAL RESULT AND DISCUSSION

Experiments have been conducted to examine the properties of fresh concrete, which were used to determine the mix ratio, strength test to determine the compressive strength and also structural tests are done to determine the performance of the beams under load. The earlier one is presented in previous chapter. So, only, the latter two tests are going to be dealt under this chapter.

4.1 Strength test

After twenty eight days the compressive strength of each cube were tested and there appears some discrepancy with the first mix ratio estimation, but the difference between the two mixes (batches) was insignificant. And since the main concern of the research is not concrete strength, the result has been adopted.

Table 4.1 ***The 28th day compressive strength of the concrete for each mix (batches)***

	PL 40/80	PL 120/CL
Test 1	31.79	32.69
Test 2	33.5	32.71
Test 3	34.03	32.53
Average	33.1	32.64

4.2 Structural test

This section presents the load carrying capacity and the failure mechanism of the control, fully bonded, beam and partially unbonded beams. The relative shear strength and the crack pattern of each beam will also be discussed.

Figure 4-1 ***beam test setup***

4.2.1 Control beam-fully bonded beam (CB)

Here the beam is assumed to be fully bonded that the reinforcement steel and the concrete is in direct contact throughout the length of the beam. This beam is a control beam which is prepared to see how much externally applied load would be resisted by fully bonded beam before it failed by shear.

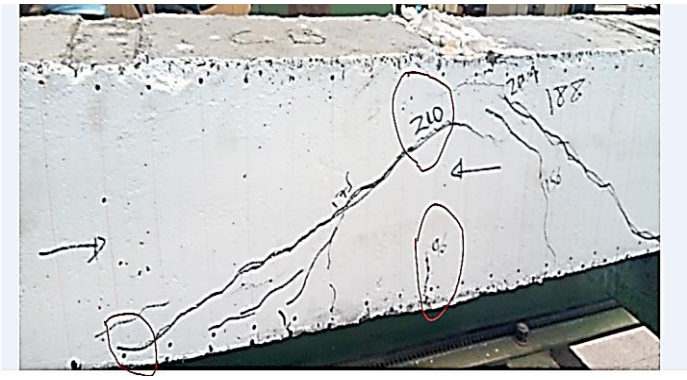

Figure 4-2 ***control beam at failure***

The failure load of the control beam is 209.58kN and the corresponding deflection is 2.45mm. It failed, as expected, by shear. The cracking pattern of this control specimen is shown in figure 4.2 where the first flexural (vertical) crack appears near the mid span at 96kN load. With the increasing load inclined crack were observed around the right support at a load of 156kN and the upper end of this crack extended towards the load point. Finally a wide inclined crack, by which the beam fails, appears at the other end extending from the support to the load point, at a load of 209.58kN, the starting point of this diagonal tension crack is somehow a few centimeter away from the support and it ends right below the loading point, but not at the support point as shown in figure 4.2.

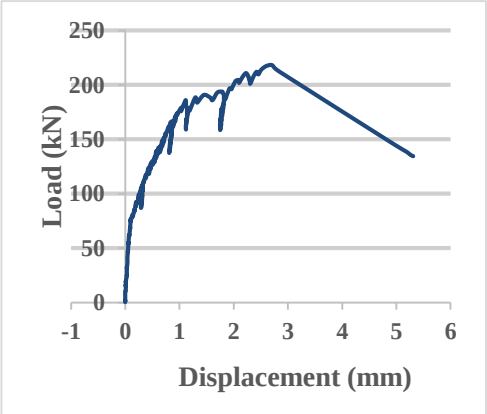

Figure 4-3 ***Load-Deflection curve for CB***

4.2.2 Beam with 40cm unbonded length (PL40)

This beam has partially unbonded 40cm length right at the mid span (20cm to the right and 20cm to the left of the center line), along which the reinforcement steel bar is not in direct contact with the concrete. The reinforcement steel bar is inserted in a pipe to blocks its contact with the concrete. The inclined cracking load and the failure load of this beam is 164kN & 210.33kN respectively. The deflection at the ultimate load is 2.13mm. This one also failed by shear. Here, also, the first vertical flexural crack appears at the mid span where the reinforced concrete beam experiences the maximum bending moment. But, Due to the complete elimination of bond within the partial length (at the mid span), radical change was observed in the first cracking load. The crack starts at very low load i.e. 50kN.

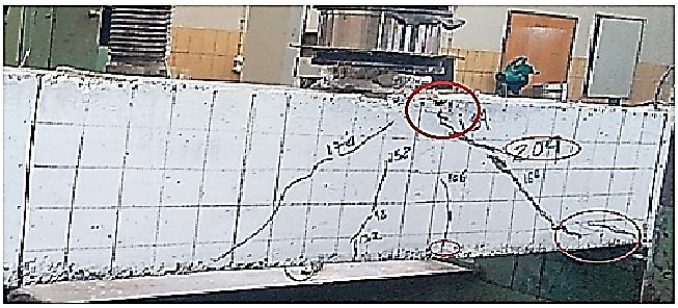

Figure 4-4 ***PL_40 at failure***

Then some web cracks appears. With the increase in load the vertical crack propagates to around the mid height then a diagonal crack occurred at one end. Later a wide diagonal crack appeared at the other end which fails the beam. Here the pattern of the crack is somehow different from the control beam. First the cracks are less in number and the failure crack also starts somehow closer to the support and ends right under the load.

4.2.3 Beam with 80cm unbonded length (PL80)

The unbonded length of the reinforcement steel in this beam specimen is 80cm. 40cm to the left and right from the center of the beam is not in direct contact with the concrete. Here also the reinforcement steel is inserted in pipe to simulate loss of bond.

Now, alike to the previous beam samples this one also fails by shear but the failure load increased to 257.35kN and the corresponding deflection is 3.32mm. The first vertical flexural crack appears at 50kN and without any other shear crack, this crack extends direct to the load point then at 210kN a shear crack has been noticed around the top part of the beam, which finally aligned with the failure crack.

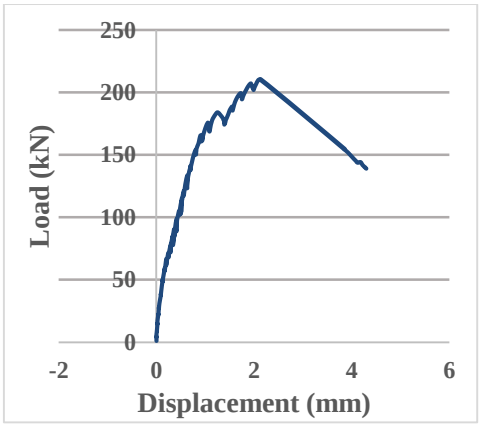

Figure 4-5 ***Load-Deflection curve for PL_40***

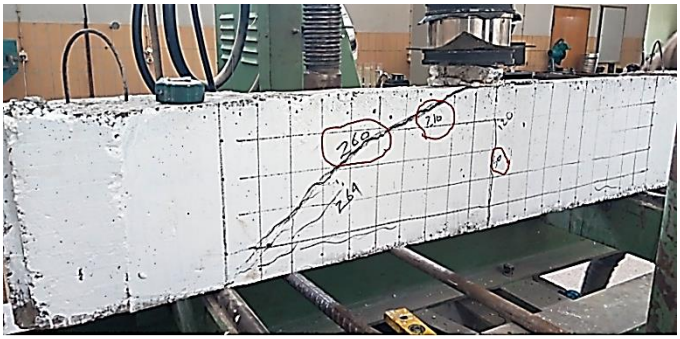

Figure 4-6 ***PL_80 at failure***

For the test specimens with partially unbonded length of 80cm, the cracking patterns were different from that of the control RC test specimen. Here, unlike the previous specimens, only flexure crack and failure crack has been observed and also the failure crack starts right from the support point and ends exactly at the loading point.

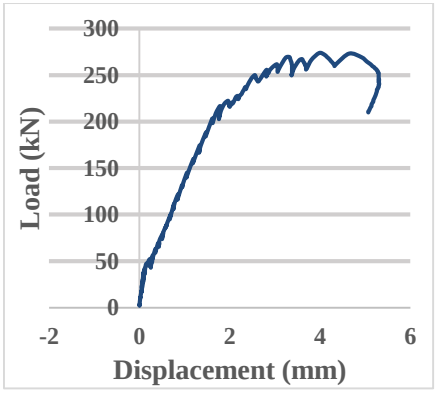

Figure 4-7 ***Load-Deflection curve for PL_80***

4.2.4 Beam with 120cm unbonded length (PL120)

The reinforcement, from support to support, in this beam specimen is unbonded with the

concrete. This is to simulate the effect of loss of bond on shear strength when the contact between the reinforcement and the concrete is totally lost.

Figure 4-8 ***PL_120***

The necessary load to prompt the first vertical flexural crack is lower than the previous specimens, and it is 34kN. This vertical crack extends upward to the compression zone as the load increased. Unfortunately without any further crack the load reaches 300kN, beyond which, the used jack is not effective, so the test stopped. But one crucial thing was observed and it is that the shear strength of this specimen is greater than 300kN, which is larger than the failure load of the other specimens.

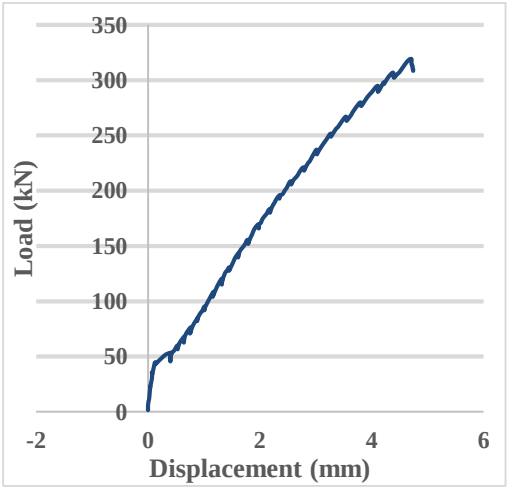

Figure 4-9 ***Load-Deflection curve for PL_120***

Figure 4.10 shows the combined load-deflection curve of all beams. As it is shown beams with longer unbonded length fails at a higher load and when the unbonded length is somehow shorter the shear behavior of the specimens becomes similar to the control fully bonded one.

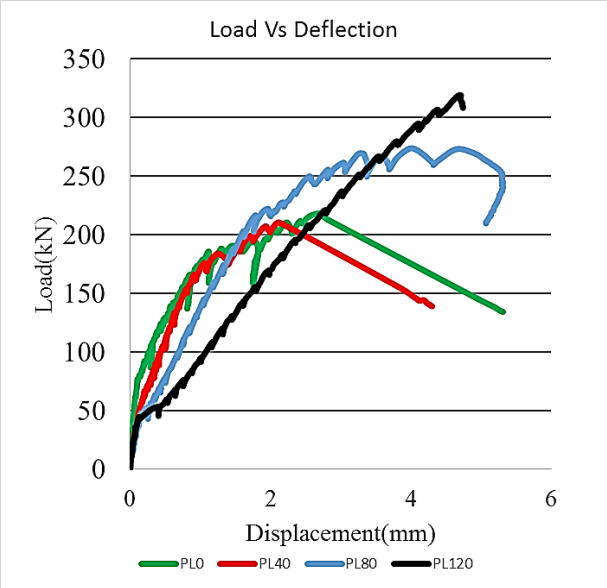

Figure 4-10 ***Combined Load-Deflection curve for all beam specimen***

As it is mentioned earlier the shear flow on the reinforced concrete is attained by the change in tension force between two points. In order, this change, to occur there must be a bond between the reinforcement steel and the concrete. This bond could be lost due to fatigue, corrosion or some other means, and once it is gone the tension force between the ends of the partial length become the same and the change will obviously be zero. A diagonal tension crack occurs as a result of the combined effect of the flexure and shear stress, and if the bond between the reinforcement steel and the concrete is lost, no shear stress would be there. So the beam will only experience vertical/ flexure/ crack or the beam will fail in arch action.

Unbonding of the longitudinal reinforcement changed the load transfer mechanism of the beams from beam action or combination of beam and arch action (control beam) to pure arch action (unbonded beams). Shear force in RC beams can be transferred by beam action or arch action depending on whether the reinforcing steel is bonded or unbonded. The reinforcement in the control (fully bonded) beam was bonded along the beam length while in the unbonded beams the reinforcement lost direct contact from the concrete due to the inserted pipe. The deboning of the reinforcement led to change in the load transfer mechanism to pure arch action in unbonded beams.

Unbonding of the longitudinal reinforcement altered the shear cracking behavior of the tested beams; the control beam experienced somehow a shorter inclined cracking, while the unbonded beams have longer inclined cracking. This phenomenon resulted in load being transferred directly from the load point to the support through arch action.

Unbonding of the longitudinal steel also changed the failure mode in the unbonded beams as compared to the control fully bonded beam. The control fully bonded beam failed in splitting of the compression struts whereas the partially 40mm unbonded beam failed in shear compression & the partially 80mm unbonded beam failed in splitting of the compression struts. According to this thesis the effect of loss of bond on shear capacity is larger on longer unbonded length.

All beams (the control fully bonded and partially unbonded beams except PL_120) failed in shear as expected. The load transfer mechanism changed from a combination of beam and arch action to pure arch action as a result of debonding of the longitudinal reinforcement. The control fully bonded beam carried 83.33% load by beam action and 16.67% load by arch action. The change in load transfer mechanism occurred at the onset of the main shear crack. Because, once the diagonal crack appears the shear flow between the main reinforcement and the compression zone is disrupted. The propagation of the inclined crack towards the compression zone was stopped by the stirrups, which helped in the development of arch action to carry the additional load until failure.

For the other specimens, the shear flow between the main reinforcement and the compression zone is already avoided due to debonding. The debonding of the longitudinal reinforcement prior to loading changed the load transfer mechanism and the beam carried 100% load by arch action. In contrast, the control fully bonded beam carried 16.67% of the load by arch action and as such the load was not affected by loss of bond.

The deflection at the ultimate load in the unbonded beams was higher compared to the control fully bonded beam. The stiffness reduction in all beams occurred at the onset of flexural cracking and the inclined cracking but larger unbonded length specimen exhibited higher reduction in stiffness. Figure 4.10 shows that the unbonded beams experienced a significant loss of stiffness after cracking. But the PL_40 specimen, relatively, shows lower stiffness reduction.

The strength increment with the partial length increment mainly attributed with the length of the required failure crack. When the beam is fully bonded the shear flow exists and the beams have a few vertical cracks around mid-span, where the shear stress is minimum, and after a while the diagonal crack occurs. But for the other beams, the loss of bond, prompt the absence of shear flow in the beams and since concrete is weak in tension, before the diagonal crack

appears the vertical cracks propagate to the next weakest, where there is a maximum moment, portion of the beam. In the course of this propagation the occurrence of diagonal crack delays and it becomes longer with the increment of the partial length which, in turn, requires higher shear force.

Table 4.2 ***Summary of unbonding effect on shear behavior of RC beams***

Beam	fck,cube	Unbonded Length (mm)	Inclined Cracking Load (kN)	Ultimate Load (kN)	Deflection at Ultimate Load (mm)	Failure Mode
PL_0	32.64	-	156	209.58	2.45	Splitting of strut
PL_40	33.1	40	164	210.35	2.13	Shear compression
PL_80	33.1	80	210	257.35	3.32	Splitting of strut
PL_120	32.64	120	-	>300	-.	-

4.3 Analysis output

The experimental result were compared to 4 different FEM model. Of which one was fully bonded, and the rest were subjected to unbond between steel and surrounding concrete. The values of the ultimate shear strength, as well as the load vs deflection curve, were obtained from the experiment and compared to the values obtained from the FEM model. Fig. 4.11 shows a comparison between the values of the ultimate strengths obtained by the experimental tests and the FEA model, while Fig. 4.12 shows the crack pattern of FEA model.

The ultimate shear strength of the control beam obtained from analysis is almost equivalent to the experimental one and pre-peak behavior also resembles with the experimental result. Bearing in mind the brittle failure mode observed during the load test, the ductility behavior beyond ultimate strength seems to be irrational and this irrational behavior of the experiment is thought to be caused by the load-applying method, so it should be noted that the post-peak behavior described by the analytical output is more reasonable.

Regarding the unbonded RC models, the ultimate shear strength of PL_40 (40cm unbonded length) is a bit larger in analysis output but there is also little change in the pre peak load-displacement graph between the experiment and the analysis. The ultimate strength and the load-displacement relationship obtained from experiment for PL_80 (80cm unbonded length)

coincides with that of analysis results. In the analysis output, the ultimate strength of PL_120 (120cm unbonded length) is revealed to be 307kN. It has been observed in the experiment that the capacity of this specimen was larger than 300kN. Here the load-displacement relationship looks somehow stiffer in the analysis result.

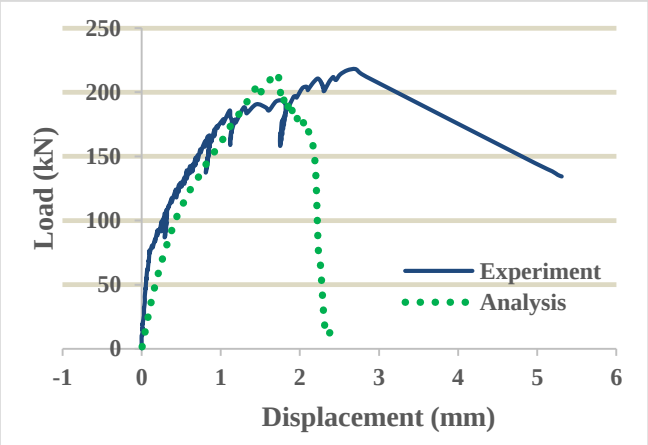

a) Control beam (PL_0)

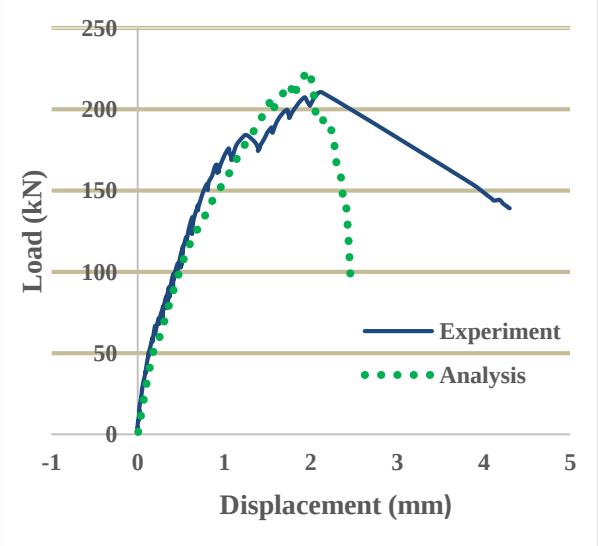

b) 40cm unbonded beam (PL_40)

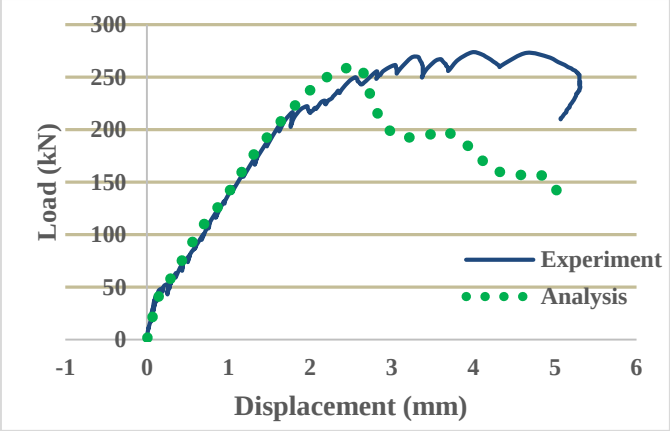

c) 80cm unbonded beam (PL_80)

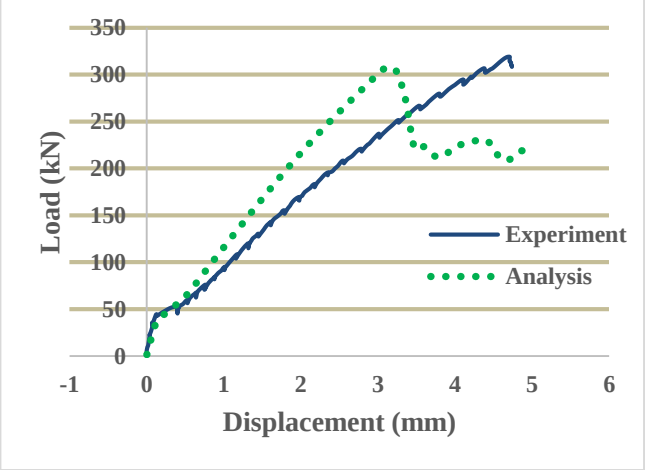

d) 120 unbonded beam (PL_120)

Figure 4-11 ***Comparison between experimental and analysis result***

As for the crack pattern at failure, the analytical output closely agrees with experimental results in control beam and also in unbonded beams. The starting point of the failure crack was getting closer to the support and the end point becomes nearer to the loading point as the partial length increases.

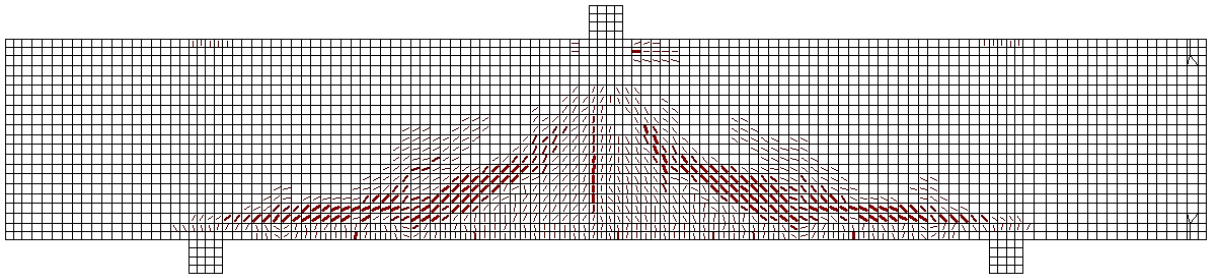

a) Control beam (PL_0)

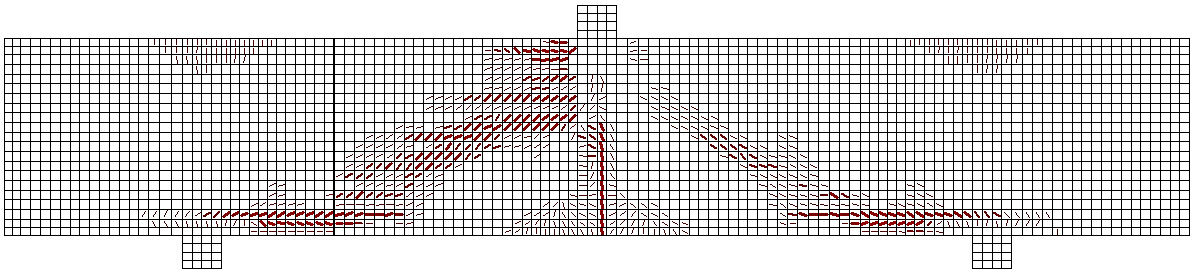

b) 40cm unbonded beam (PL_40)

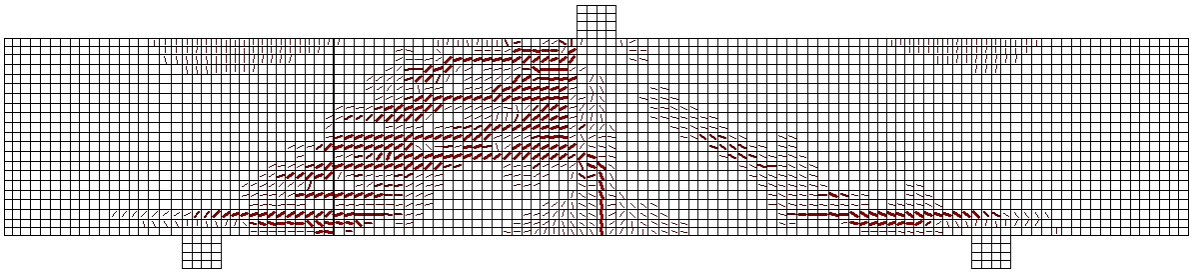

c) 80cm unbonded beam (PL_80)

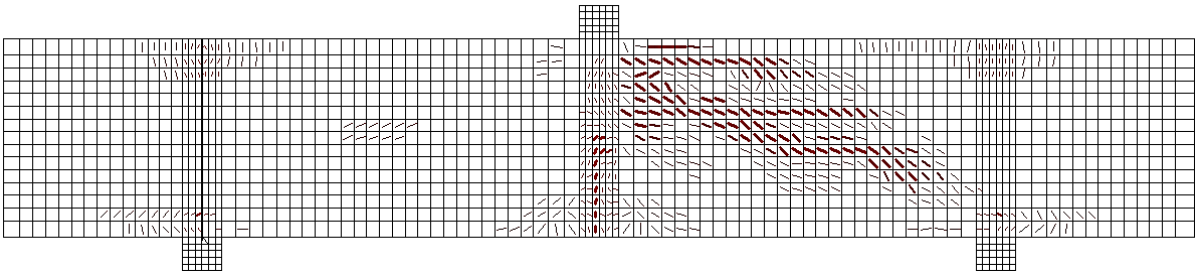

d) 120cm unbonded beam (PL_120)

Figure 4-12 ***Crack pattern from FEM***

CHAPTER 5 CONCLUSIONS AND RECCOMENDATIONS

5.1 Conclusion

The result for the four beam specimen shows that the shear capacity as well as the pattern of the cracks varies. Based on experimental data and Finite element analysis of the control fully bonded beam and unbonded beams the following conclusions were drawn.

i. The shear resistance for lower unbonding length (PL_40) shows insignificant change but for larger unbonded length (PL_80 and PL_120) it increases in a higher rate. From this it can be concluded that loss of bond between the reinforcement and concrete, providing the reinforcement is anchored adequately, don't adversely affect the shear capacity. The result summarized in the table below.

Table 5.1 ***Failure load of specimens***

Partial length (cm)	Failure load (kN)
0	209
40	210
80	260
120	>300

ii. The required force to induce first vertical flexural crack is inversely proportional to the unbonded length and the number of cracks also get lower and lower as the partial length increases. The starting point of the failure crack was getting closer to the support and the end point becomes nearer to the loading point as the partial length increases. The beams are also observed to be ductile as the partial unbonding length increases

iii. The pre-peak load deflection curve and the crack pattern from experiment is very close to the result from analysis for the fully bonded control beam and the two (PL_40 & PL_80) beam specimens. But for the last specimen (PL_120) the result from the analysis is somehow stiffer than the experiment one.

5.2 Recommendation

- The increment in shear capacity was observed only for larger unbonded length, but for the unbonded 40mm length (PL_40) the increment is insignificant relative to the control beam, which holds back the thesis to generalize the effect of loss of bond on shear strength for shorter unbonded length. So to see the effect in shorter unbonded length, the number of sample should be more.

- Mathematical Relation between the increment in shear capacity and loss of bond can be made, if the specimen number were larger and the unbonded length interval less.

- There is a little discrepancy between the experiment result and analysis output. This discrepancy could be a result of somehow larger mesh size, which was in fact the limiting size for Vector 2, using better FE software could yield closer result with experimental one.

REFERENCES

1. P. S. Wong, F.J. Vecchio & H. Trommels, "Vector2 & Formworks User's Manual" second edition, August, 2013.

2. Xiao-Hui Wang & Xi-la Liu, "Shear behavior of RC beams with corrosion damaged partial length", Article in Materials and Structures,· March 2011.

3. James K. Wight & James G. Macgregor, "Reinforced Concrete Mechanics and Design" Sixth edition, 2011.

4. Xiao-Hui Wang & Xi-la Liu, "Predicting the flexural capacity of RC beam with partially unbonded steel Reinforcement", Article in Computers and Concrete, June 2009.

5. Vu Hiep Dang, Raoul François & Dario Coronelli, "Shear behaviour and load capacity of short reinforced concrete beams exposed to chloride environment", European Journal of Environmental and Civil Engineering, 27 Apr 2015.

6. Ethiopian Building Code Standard, "Design of Concrete Structures (EBCS EN 1992-1-1:2013)", 2013.

7. Kyle Stanish, "Corrosion Effects on Bond Strength in Reinforced Concrete", University of Toronto, 1997.

8. Xiao-Hui Wang & Xi-la Liu, "Predicting the flexural capacity of RC beam with partially unbonded steel Reinforcement", June 2009.

9. Vu Hiep Dang, Raoul François & Dario Coronelli, "Shear behaviour and load capacity of short reinforced concrete beams exposed to chloride environment", European Journal of Environmental and Civil Engineering, 27 Apr 2015.

10. Xin Xue1 and Hiroshi Seki, "Influence of Longitudinal Bar Corrosion on Shear Behavior of RC Beams", Journal of Advanced Concrete Technology, April 2010.

11. Rizwan Azam, "Behaviour of Shear Critical RC Beams with Corroded Longitudinal Steel Reinforcement", Waterloo, Ontario, Canada, 2010.

APPENDIX A

Mix ratio

Procedure for Concrete Mix Design of M25 Concrete

Step 1 — Determination of Target Strength

Himsworth constant for 5% risk factor is 1.65. In this case standard deviation is taken from IS:456 against M 25 is 4.0.

$f_{target} = f_{ck} + 1.65 \times S$

$= 25 + 1.65 \times 4.0 = 31.6\ N/mm^2$

Where,

S = standard deviation in N/mm^2 = 4 (as per table -1 of IS 10262- 2009)

Step 2 — Estimation of mixing water

Depends on: - maximum nominal aggregate size

Particle shape

Grading of aggregates

The estimated mixing water is 186kg/m^3

Step 3 — Selection of water / cement ratio:-

-strength

-durability

-finishabilty

Maximum water-cement ratio for Mild exposure condition = 0.55

Adopt 0.5<0.55, hence OK.

Step 4 — calculation of cement content

Water-cement ratio = 0.5

Corrected water content = 186kg /m^3

Cement content =186/0.5=372kg

Minimum cement Content for mild exposure condition = 300 kg/m^3

372 kg/m^3 > 300 kg/m^3, hence, OK.

Step 5-Estimation of coarse aggregate content

-Nominal maximum aggregate size

-fineness modulus of FA

- And For w/c = 0.5

Volume of coarse aggregate per unit volume of total aggregate = 0.604

Step 6-Estimation of fine aggregate content

Volume of fine aggregate = 1 – 0.604 = 0.396

Step 7- Estimation of the mix ingredients

Volume of concrete = 1 m^3

Volume of cement = (Mass of cement / Specific gravity of cement) x (1/100)

= (372/3.15) x (1/1000) = 0.1181 m^3

Volume of water = (Mass of water / Specific gravity of water) x (1/1000)

= (186/1) x (1/1000) = 0.186 m^3

Volume of total aggregates = 1 – (0.1181 + 0. 186) =0.696 m^3

Mass of coarse aggregates = 0. 696 x 0.604 x 2.67 x 1000 =1122.27 kg/m^3

Mass of fine aggregates = 0. 696 x 0.396 x 2.61 x 1000 = 719.26 kg/m^3

Concrete Mix proportions for Trial Mix 1

Cement = 372 kg/m^3

Water = 186 kg/m^3

Fine aggregates = 719.26kg/m^3

Coarse aggregate = 1122.27kg/m^3

W/c = 0.5

For trial -1 casting of concrete in lab, to check its properties.

For casting trial -1, mass of ingredients required will be calculated for 6 no's cube assuming 25% wastage.

Volume of concrete required for 6 cubes = 6 x (0.15^3 x1.25) = 0.0244 m^3

Cement = (372×0.0244) kg/m^3 = 9.1 kg

Water = (186 x 0.0244) kg/m^3 =4.6 kg

Coarse aggregate = (1122.27 x 0.0244) kg/m^3 =27.4 kg

Considering 20 mm: 10mm = 0.55: 0.45

Coarse aggregate 20 mm = 15.1 kg
Coarse aggregate 10 mm =12.4 kg

Fine aggregates = (719.26 x 0.0244) kg/m^3 = 17.6 kg

With this proportion, concrete is manufactured and tested for fresh concrete properties requirement i.e. workability,

In this case,

Slump value = 15 mm

Desired slump = 50-75 mm

So modifications are needed in trial mix 1 to arrive at the desired workability.

Concrete Trial Mix 2:

To increase the workability from 25 mm to 50-75 mm an increase in water content by 3% is to be made.

The corrected water content = 186x 1.03 = 191.08 kg.

As mentioned earlier to adjust fresh concrete properties the water cement ratio will not be changed. Hence

Cement Content = (199.02/0.5) = 382.16 kg/m^3

Volume of all aggregate = 1 – [{382.16/ (3.15×1000)} + {191.08/ (1 x 1000)}] = 0.6746 m^3

Mass of coarse aggregate = 0.6746 x 0.604 x 2.67 x 1000 = 1108.88 kg/m^3

Mass of fine aggregates = 0.6746 x 0.396 x 2.61 x 1000 = 710.67 kg/m^3

Concrete Mix Proportions for Trial Mix 2

Cement = 382.16 kg/m^3

Water = 191.08 kg/m^3

Fine aggregate =710.67 kg/m^3

Coarse aggregate = 1108.88 kg/m^3

For casting trial -2, mass of ingredients required will be calculated for 6 no's cube assuming 25% wastage.

Volume of concrete required for 6 cubes = 6 x (0.15^3 x1.25) = 0.025313 m^3

Cement = (382.16x 0.025313) kg/m^3 = 9.7 kg

Water = (191.08x 0.025313) kg/m^3 =4.9 kg

Coarse aggregate = (1108.88 x 0.025313) kg/m^3 =28.1 kg

Fine aggregates = (710.67 x 0.025313) kg/m^3 = 18 kg

In this case,

Slump value = 55 mm

And did not exhibit any segregation and bleeding.

Desired slump = 50-75 mm

So, it has achieved desired workability by satisfying the requirement of 50-75 mm slump value.

Cement: F.A: C.A=1:1.9:3

With this proportion the third day compressive strength for three cube test is 13.22 MPa, 14.47 MPa, and 15.98 MPa. The average of these is **14.56 MPa** which is ***58.24%*** of the 28^{th} day strength, so it is accepted.

Load vs Deflection

From Experiment

Control beam(PL0)		Beam with 40cm unbonded length (PL40)		Beam with 80cm unbonded length (PL80)		Beam with 120cm unbonded length (PL120)	
Load	deflection	load	deflection	load	deflection	load	deflection
0.25	0	1	0	2.25	0	1.75	0
0.5	0	1	0	3.25	0	1.5	0
1.75	0	4.25	0	2.75	0	5.75	0
1.5	0	4	0	2.75	0	9.75	0.01
1.5	0	6.25	0	8	0.01	9.75	0.01
3	0	9	0.01	11.5	0.02	9.75	0.01
3	0	8.75	0.01	11	0.02	11.75	0.02
4.25	0	8.75	0.01	10.75	0.02	17.26	0.03
5.75	0	9.75	0.01	11.5	0.02	22.76	0.04
5.75	0	14.51	0.02	17.01	0.04	23.01	0.04
10.25	0	14.76	0.02	19.26	0.05	22.51	0.04
10.5	0.01	14.51	0.02	18.26	0.05	23.01	0.04
13.76	0.01	17.01	0.02	17.76	0.05	30.26	0.07
16.01	0.01	22.51	0.04	17.26	0.05	35.76	0.07
15.51	0.01	22.26	0.04	21.01	0.05	34.76	0.07
15.51	0.01	22.01	0.04	23.51	0.05	34.01	0.08
15.26	0.01	22.01	0.04	23.51	0.06	34.76	0.08
15.01	0.01	27.76	0.05	21.76	0.06	44.27	0.12
19.26	0.01	27.01	0.05	21.01	0.05	44.77	0.13
18.76	0.01	27.01	0.05	26.51	0.06	43.27	0.13
25.26	0.03	31.01	0.06	27.26	0.07	42.77	0.13
24.26	0.03	37.77	0.09	24.76	0.06	42.77	0.13

32.01	0.03	38.52	0.09	23.51	0.06	50.77	0.29
31.51	0.03	38.02	0.09	26.51	0.06	53.27	0.4
36.01	0.04	37.77	0.09	31.26	0.08	50.52	0.41
39.52	0.04	38.27	0.09	27.51	0.08	49.52	0.4
41.02	0.04	45.02	0.11	33.26	0.09	48.77	0.4
47.27	0.05	50.77	0.13	30.01	0.08	48.27	0.4
46.52	0.05	50.02	0.13	29.01	0.07	48.02	0.4
55.27	0.06	49.52	0.13	38.02	0.09	47.77	0.4
53.77	0.06	49.02	0.13	33.76	0.09	47.27	0.4
62.02	0.07	48.77	0.13	32.26	0.09	47.27	0.4
61.27	0.08	48.52	0.13	40.02	0.1	47.02	0.4
62.78	0.08	50.02	0.13	42.27	0.12	46.77	0.4
69.03	0.09	54.77	0.15	39.27	0.12	46.52	0.4
67.78	0.09	59.52	0.17	37.51	0.12	46.27	0.4
76.53	0.1	58.02	0.17	36.01	0.11	46.27	0.4
74.28	0.1	57.02	0.17	46.27	0.14	46.02	0.4
80.28	0.13	57.02	0.17	48.52	0.19	46.02	0.4
79.53	0.14	66.78	0.2	45.52	0.19	45.77	0.4
78.78	0.14	64.03	0.2	51.27	0.21	45.77	0.4
85.53	0.17	62.53	0.2	53.27	0.28	45.52	0.4
83.53	0.17	61.77	0.2	50.77	0.27	45.52	0.4
92.29	0.2	61.52	0.2	56.27	0.29	49.52	0.4
88.29	0.2	71.28	0.24	54.02	0.29	53.52	0.43
89.54	0.2	71.53	0.26	52.27	0.28	55.52	0.47
93.54	0.23	69.03	0.25	50.77	0.28	58.27	0.5
91.54	0.23	68.03	0.25	49.52	0.28	59.77	0.52

99.04	0.25	72.53	0.26	48.52	0.27	59.77	0.53
95.29	0.25	79.28	0.3	47.27	0.26	58.52	0.53
93.29	0.25	74.28	0.29	46.27	0.26	57.52	0.53
91.54	0.25	72.78	0.29	45.52	0.25	57.02	0.53
99.79	0.26	72.03	0.29	44.52	0.25	56.52	0.53
97.54	0.26	75.78	0.29	43.77	0.25	62.02	0.56
95.54	0.26	85.03	0.33	43.52	0.25	66.28	0.62
93.54	0.25	80.78	0.32	43.02	0.25	67.78	0.64
102.29	0.28	79.03	0.32	46.52	0.25	66.78	0.64
100.79	0.28	79.03	0.32	49.52	0.26	64.78	0.64
99.04	0.28	90.54	0.36	48.77	0.26	63.78	0.64
96.79	0.28	82.78	0.35	48.27	0.26	63.03	0.64
105.29	0.29	79.28	0.34	63.03	0.35	62.53	0.64
104.04	0.3	77.78	0.34	60.52	0.35	62.53	0.64
102.04	0.3	86.53	0.36	59.02	0.35	68.53	0.66
99.79	0.3	90.29	0.38	69.28	0.41	73.78	0.72
107.79	0.31	87.54	0.38	69.28	0.44	76.28	0.76
106.79	0.32	85.78	0.37	67.28	0.43	75.78	0.76
105.04	0.32	84.78	0.37	65.53	0.43	73.78	0.76
103.04	0.32	85.03	0.37	72.03	0.44	72.78	0.76
101.04	0.31	91.04	0.38	80.03	0.52	71.78	0.76
98.79	0.31	98.54	0.41	76.78	0.51	71.28	0.75
97.04	0.31	96.29	0.42	75.28	0.5	70.78	0.75
95.29	0.31	94.29	0.41	73.78	0.5	77.78	0.8
93.79	0.31	93.04	0.41	81.53	0.53	82.78	0.86
92.04	0.3	92.04	0.41	88.79	0.6	84.28	0.88

90.29	0.3	91.04	0.41	86.03	0.58	84.53	0.88
88.54	0.3	90.29	0.41	90.54	0.61	84.28	0.88
86.78	0.29	89.79	0.41	100.29	0.69	84.28	0.88
93.54	0.3	89.29	0.41	96.54	0.67	82.78	0.88
93.04	0.3	88.79	0.41	95.04	0.67	82.03	0.88
91.54	0.3	95.04	0.41	111.04	0.76	83.78	0.88
91.04	0.3	105.04	0.46	107.54	0.76	88.79	0.93
98.79	0.31	105.04	0.47	105.79	0.75	91.29	0.97
97.54	0.31	103.29	0.47	111.54	0.77	93.79	0.99
96.04	0.31	101.79	0.47	121.55	0.85	95.04	1.01
106.04	0.32	103.79	0.47	118.8	0.85	95.29	1.01
104.54	0.32	115.3	0.52	117.05	0.85	93.29	1.01
103.04	0.32	112.04	0.52	116.05	0.84	92.54	1.01
106.79	0.32	109.54	0.51	131.55	0.94	91.79	1.01
111.29	0.34	107.79	0.51	131.3	0.95	94.54	1.02
110.04	0.34	106.54	0.51	129.55	0.95	104.29	1.12
110.04	0.34	105.79	0.51	131.3	0.95	108.54	1.17
117.3	0.38	104.79	0.51	145.06	1.05	106.54	1.17
115.3	0.38	104.04	0.5	142.56	1.05	105.04	1.16
114.05	0.38	103.54	0.5	141.06	1.05	104.04	1.16
123.8	0.43	103.04	0.5	139.81	1.04	104.29	1.16
121.05	0.43	102.79	0.5	144.31	1.07	112.8	1.23
119.05	0.43	113.3	0.52	159.56	1.19	120.05	1.31
118.05	0.44	121.3	0.56	156.81	1.19	119.8	1.33
127.55	0.47	119.05	0.56	155.31	1.18	117.8	1.32
124.3	0.47	118.05	0.56	155.06	1.18	116.55	1.32

122.55	0.47	117.3	0.56	174.32	1.33	115.55	1.32
128.05	0.48	126.3	0.59	172.82	1.34	115.05	1.32
129.55	0.5	133.55	0.63	171.07	1.34	119.3	1.33
127.05	0.51	130.8	0.63	169.82	1.33	123.3	1.36
126.3	0.5	129.55	0.63	169.07	1.33	125.8	1.38
133.3	0.54	128.55	0.63	167.82	1.33	128.3	1.42
130.8	0.54	127.55	0.63	167.32	1.32	130.3	1.44
128.55	0.54	127.05	0.63	166.57	1.32	130.55	1.45
139.06	0.57	126.55	0.63	172.07	1.34	130.3	1.45
136.05	0.57	126.05	0.63	188.08	1.47	129.05	1.45
133.8	0.57	125.3	0.63	185.57	1.47	128.05	1.45
132.55	0.57	124.8	0.63	184.07	1.47	127.55	1.45
142.06	0.61	124.55	0.63	184.57	1.47	130.8	1.48
139.31	0.61	124.05	0.63	203.08	1.61	135.05	1.52
136.8	0.61	123.8	0.63	201.08	1.62	139.56	1.56
140.81	0.62	123.3	0.63	199.33	1.62	143.06	1.61
143.81	0.65	123.8	0.62	198.33	1.62	143.31	1.61
141.06	0.65	133.05	0.65	208.83	1.69	141.56	1.61
138.06	0.64	139.56	0.69	216.59	1.78	140.56	1.61
148.56	0.68	141.31	0.7	213.09	1.78	140.06	1.61
145.81	0.68	140.06	0.69	211.33	1.78	139.56	1.61
143.56	0.68	139.06	0.7	209.83	1.77	143.81	1.63
143.06	0.68	138.56	0.69	208.58	1.77	146.81	1.66
151.06	0.71	138.06	0.7	207.58	1.77	148.56	1.69
149.06	0.71	137.81	0.69	206.83	1.77	152.06	1.74
147.06	0.71	144.81	0.73	206.08	1.77	154.56	1.76

155.31	0.74	149.56	0.76	205.58	1.77	155.56	1.78
154.81	0.75	154.06	0.8	204.83	1.76	155.06	1.79
153.06	0.75	153.56	0.81	204.33	1.76	154.06	1.79
153.81	0.75	152.31	0.81	204.08	1.76	153.31	1.79
161.56	0.8	151.31	0.81	203.58	1.76	152.56	1.79
159.06	0.8	150.81	0.81	203.08	1.76	152.06	1.79
157.56	0.8	150.31	0.81	202.83	1.76	151.81	1.79
164.82	0.83	155.06	0.82	202.58	1.76	157.31	1.83
166.32	0.86	159.06	0.86	211.08	1.8	160.31	1.86
164.32	0.86	162.57	0.88	219.09	1.88	163.07	1.88
162.31	0.86	165.57	0.9	222.34	1.96	166.82	1.92
160.31	0.86	165.82	0.92	219.84	1.97	169.57	1.97
157.56	0.86	164.32	0.92	218.59	1.98	169.07	1.98
155.56	0.85	163.57	0.92	217.84	1.98	168.07	1.98
153.31	0.85	162.82	0.92	217.34	1.99	167.32	1.98
151.06	0.85	162.06	0.92	216.59	1.99	166.82	1.97
148.81	0.84	161.81	0.92	215.84	2	166.07	1.98
146.81	0.83	161.31	0.92	216.34	2	165.82	1.98
144.81	0.83	160.81	0.92	217.59	2.02	168.82	1.98
142.81	0.83	164.57	0.94	218.09	2.03	170.57	2.01
139.81	0.82	163.82	0.94	218.84	2.04	171.07	2.02
137.3	0.81	163.07	0.94	220.34	2.05	174.82	2.05
149.06	0.83	162.57	0.94	220.84	2.07	179.07	2.12
147.31	0.83	162.06	0.94	219.84	2.07	182.07	2.15
144.81	0.83	161.56	0.94	219.59	2.07	183.57	2.18
155.31	0.85	163.32	0.94	222.59	2.1	182.07	2.18

153.31	0.85	171.32	1	224.84	2.12	181.32	2.18
150.81	0.84	175.82	1.05	226.59	2.14	180.57	2.18
161.06	0.86	174.07	1.06	227.34	2.16	180.07	2.18
159.81	0.86	173.07	1.06	227.59	2.17	184.57	2.21
157.56	0.86	172.32	1.07	227.59	2.18	189.08	2.26
162.06	0.87	171.82	1.07	226.84	2.18	193.58	2.31
165.57	0.89	171.07	1.08	226.09	2.18	195.83	2.35
163.57	0.89	170.57	1.08	225.34	2.18	195.58	2.35
161.31	0.88	170.07	1.08	224.84	2.18	194.58	2.35
170.82	0.92	169.82	1.08	224.59	2.18	193.83	2.35
168.32	0.92	169.32	1.08	224.34	2.19	193.08	2.35
165.82	0.92	169.07	1.08	224.09	2.19	192.83	2.35
172.32	0.94	168.82	1.09	225.34	2.2	195.33	2.36
173.82	0.96	171.32	1.1	226.59	2.21	197.08	2.41
172.07	0.96	177.82	1.14	228.34	2.23	199.83	2.44
172.82	0.96	182.57	1.21	228.59	2.24	202.58	2.48
178.82	1.03	184.07	1.26	229.59	2.26	205.83	2.51
176.82	1.03	180.07	1.35	230.34	2.27	208.33	2.54
175.57	1.03	178.57	1.37	231.59	2.28	208.08	2.56
185.57	1.11	178.07	1.38	234.84	2.32	207.08	2.56
182.57	1.12	177.32	1.38	237.09	2.34	206.58	2.56
181.07	1.12	177.07	1.39	236.34	2.35	205.83	2.56
179.57	1.13	176.57	1.39	235.59	2.35	205.58	2.56
177.82	1.14	176.32	1.39	235.09	2.36	209.58	2.6
176.07	1.14	175.82	1.39	234.84	2.36	211.33	2.63
174.07	1.14	175.57	1.39	238.6	2.39	213.59	2.67

172.32	1.14	175.32	1.39	246.35	2.48	217.09	2.71
170.82	1.14	175.07	1.39	249.85	2.55	219.34	2.74
169.07	1.14	174.82	1.39	248.85	2.57	220.59	2.76
167.07	1.13	174.57	1.39	247.1	2.58	221.09	2.78
164.82	1.13	174.32	1.39	246.1	2.58	220.84	2.79
162.57	1.12	174.32	1.39	245.1	2.6	219.84	2.79
160.56	1.12	175.07	1.4	244.1	2.61	219.34	2.79
158.81	1.12	176.07	1.41	243.35	2.62	218.84	2.79
163.32	1.12	178.07	1.42	243.1	2.62	218.34	2.79
168.82	1.13	178.82	1.43	243.35	2.64	218.09	2.79
167.82	1.13	181.57	1.46	244.85	2.66	222.34	2.83
167.82	1.13	183.57	1.48	246.1	2.68	225.59	2.87
178.57	1.18	185.82	1.5	247.6	2.7	226.59	2.89
177.07	1.19	187.83	1.53	249.85	2.73	230.34	2.93
176.32	1.19	188.83	1.55	252.1	2.76	234.84	2.98
188.08	1.29	187.57	1.55	254.85	2.8	237.09	3.01
185.07	1.32	187.07	1.55	255.6	2.82	236.34	3.02
183.57	1.33	186.32	1.55	253.85	2.82	235.34	3.02
190.58	1.45	186.07	1.55	252.85	2.82	234.59	3.02
188.08	1.57	185.57	1.56	252.1	2.82	233.84	3.02
185.82	1.61	190.08	1.59	251.35	2.82	233.34	3.02
192.83	1.7	194.33	1.63	250.6	2.82	233.09	3.02
193.58	1.79	198.33	1.69	250.1	2.82	232.84	3.02
192.33	1.8	199.58	1.73	249.6	2.82	235.84	3.05
191.33	1.81	197.58	1.74	248.85	2.81	239.85	3.1
190.58	1.82	196.83	1.74	248.6	2.81	242.85	3.14

189.83	1.82	196.33	1.75	248.35	2.81	246.35	3.19
189.33	1.82	195.83	1.75	248.35	2.81	251.1	3.25
188.83	1.82	195.33	1.75	251.6	2.84	251.6	3.27
188.08	1.82	195.08	1.75	252.1	2.86	250.35	3.27
187.57	1.82	194.58	1.75	254.6	2.88	249.6	3.27
186.82	1.82	195.08	1.76	256.6	2.91	249.1	3.27
185.82	1.82	196.58	1.77	259.85	2.98	248.85	3.27
184.32	1.82	199.33	1.8	261.6	3.04	255.85	3.36
183.07	1.82	202.33	1.84	260.6	3.05	257.85	3.4
181.57	1.82	205.08	1.88	259.1	3.05	263.11	3.47
180.32	1.81	207.33	1.93	258.35	3.06	266.86	3.53
178.57	1.81	205.83	1.95	257.35	3.06	266.36	3.55
176.32	1.8	204.58	1.96	256.85	3.06	265.11	3.55
174.57	1.8	203.83	1.97	255.85	3.06	264.11	3.55
173.07	1.79	203.08	1.98	255.35	3.06	263.61	3.55
171.57	1.79	202.58	1.99	254.6	3.06	263.11	3.55
170.32	1.78	202.08	1.99	253.85	3.06	268.36	3.63
168.82	1.78	207.58	2.05	253.35	3.06	271.11	3.66
167.32	1.78	210.33	2.13	258.6	3.11	278.86	3.77
166.07	1.77	154.56	3.85	268.61	3.24	279.86	3.8
164.57	1.77	147.06	4.04	269.36	3.32	278.36	3.8
163.07	1.77	145.06	4.09	267.11	3.34	277.36	3.8
161.56	1.76	143.81	4.12	265.61	3.35	276.61	3.81
160.06	1.76	144.31	4.18	264.36	3.36	277.61	3.83
158.31	1.75	142.81	4.21	263.11	3.37	284.61	3.92
166.57	1.75	142.06	4.22	262.1	3.37	289.12	4

168.82	1.76	141.31	4.24	260.85	3.38	293.62	4.07
167.82	1.76	140.81	4.25	259.85	3.38	294.87	4.11
176.32	1.77	140.56	4.26	259.1	3.38	292.62	4.11
178.07	1.78	140.31	4.27	258.1	3.38	291.62	4.11
177.32	1.78	139.81	4.28	257.35	3.38	290.87	4.11
187.83	1.84	139.81	4.28	256.6	3.38	290.37	4.11
187.57	1.85	139.56	4.28	255.85	3.38	289.87	4.11
187.07	1.85	139.31	4.29	255.1	3.38	289.37	4.11
196.33	1.92	139.06	4.3	254.35	3.38	291.37	4.14
196.83	1.96	138.81	4.3	253.6	3.38	297.87	4.21
195.83	1.96	138.81	4.3	253.1	3.38	296.62	4.22
203.08	2.03	138.56	4.3	252.35	3.38	301.62	4.28
204.33	2.08	138.31	4.3	251.6	3.38	305.37	4.34
203.33	2.09	138.31	4.3	250.85	3.38	306.87	4.38
202.33	2.1	138.06	4.31	250.35	3.37	305.12	4.39
202.08	2.1	138.06	4.32	249.85	3.37	304.12	4.39
201.58	2.1	137.81	4.32	249.6	3.37	303.12	4.39
206.83	2.16	137.81	4.32	250.35	3.37	302.62	4.39
210.58	2.22	137.55	4.32	255.85	3.41	302.37	4.4
209.58	2.25	137.3	4.32	260.35	3.46	302.12	4.4
208.58	2.26	137.3	4.33	265.86	3.54	305.62	4.46
207.83	2.27	137.3	4.34	267.11	3.6	306.87	4.49
207.08	2.27	137.05	4.39	265.61	3.62	311.12	4.55
206.58	2.28	137.05	4.36	264.61	3.63	315.38	4.61
206.08	2.28	136.8	4.33	263.86	3.64	318.63	4.67
205.83	2.28	136.8	4.33	263.11	3.65	319.13	4.71

205.33	2.29	136.55	4.33	262.61	3.66	317.63	4.71
204.83	2.29	136.55	4.33	261.85	3.66	316.63	4.71
204.58	2.29	136.55	4.33	261.1	3.67	315.88	4.71
204.33	2.29	136.3	4.33	260.35	3.67	315.38	4.71
203.83	2.29	136.3	4.33	259.85	3.68	314.88	4.71
203.58	2.3	136.3	4.33	258.85	3.69	314.38	4.71
203.33	2.3	136.05	4.33	258.1	3.69	313.88	4.72
203.08	2.3	136.05	4.34	257.6	3.69	313.38	4.72
202.83	2.3	136.05	4.33	256.85	3.69	313.13	4.72
202.58	2.3	135.8	4.34	256.6	3.69	312.62	4.73
202.33	2.3	135.8	4.34	256.1	3.69	312.37	4.73
202.33	2.3	135.8	4.34	255.85	3.69	311.87	4.73
202.08	2.3	135.55	4.34	257.35	3.71	311.37	4.73
201.83	2.3	135.55	4.34	266.36	3.81	311.12	4.73
201.58	2.3	135.55	4.34	273.61	3.98	310.87	4.73
201.33	2.3	135.3	4.34	272.11	4.09	310.62	4.73
201.33	2.3	135.3	4.34	269.61	4.15	310.37	4.73
201.08	2.3	135.3	4.34	267.86	4.19	310.12	4.73
200.83	2.3	135.3	4.34	266.36	4.22	309.87	4.74
200.83	2.3	135.3	4.34	265.11	4.24	309.62	4.74
201.08	2.31	135.05	4.34	264.11	4.26	309.37	4.74
208.08	2.37	135.05	4.34	263.11	4.28	309.12	4.74
211.83	2.42	135.05	4.34	262.35	4.29	308.87	4.74
211.08	2.43	135.05	4.34	261.35	4.31	308.62	4.74
210.33	2.44	134.8	4.34	260.35	4.32	308.37	4.74
209.58	2.45	134.8	4.34	259.6	4.32		

209.58	2.46	134.8	4.34	262.86	4.38
213.84	2.51	134.8	4.34	273.11	4.65
217.09	2.6	134.55	4.34	269.11	4.92
218.09	2.7	134.55	4.34	264.36	5.04
215.09	2.76	134.3	4.34	261.6	5.12
212.08	2.84	134.3	4.34	259.6	5.16
144.81	4.97	134.3	4.34	258.35	5.2
138.31	5.19	134.05	4.34	257.1	5.22
135.55	5.26	134.05	4.34	256.1	5.25
134.3	5.31	134.05	4.34	255.1	5.26

From FEM

Control beam(PL0)		Beam with 40cm unbonded length (PL40)		Beam with 80cm unbonded length (PL80)		Beam with 120cm unbonded length (PL120)	
Load	Deflection	Load	Deflection	Load	Deflection	Load	Deflection
1.556	0.005	1.554	0.005	1.556	0.005	1.5	0.005
9.306	0.03	9.29	0.03	38.022	0.129	36.176	0.129
16.964	0.055	16.938	0.055	54.052	0.254	45.838	0.254
24.542	0.079	24.502	0.079	68.434	0.379	54.304	0.379
32.002	0.104	31.886	0.104	85.786	0.503	63.412	0.503
39.052	0.129	38.71	0.129	101.544	0.628	76	0.629
45.622	0.154	44.918	0.154	115.494	0.752	89.368	0.753

51.748	0.179	50.652	0.179	126.884	0.877	102.724	0.878
57.524	0.204	54.24	0.204	140.38	1.002	115.912	1.003
63.042	0.228	56.418	0.229	155.318	1.127	129.052	1.127
68.3	0.254	60.222	0.254	170.316	1.251	141.838	1.252
73.366	0.278	64.64	0.278	182.738	1.376	154.92	1.377
78.244	0.303	69.11	0.304	195.544	1.501	167.754	1.502
82.956	0.328	73.668	0.328	206.568	1.626	180.316	1.626
87.53	0.353	78.148	0.354	217.516	1.751	192.62	1.751
91.98	0.378	82.59	0.378	227.868	1.875	204.596	1.875
96.264	0.403	86.926	0.403	237.497	2	216.346	2
100.4	0.428	91.194	0.428	245.73	2.126	227.786	2.125
104.316	0.453	95.374	0.453	252.012	2.253	238.89	2.25
107.32	0.477	99.488	0.478	255.384	2.38	249.718	2.374
110.79	0.502	103.532	0.503	260.999	2.51	260.158	2.499
113.606	0.527	107.462	0.528	256.222	2.641	270.39	2.623
116.722	0.552	110.844	0.553	224.231	2.775	280.414	2.748
119.8	0.577	114.05	0.577	205.69	2.905	290.439	2.872
122.73	0.602	117.03	0.602	195.491	3.031	299.948	2.996
125.266	0.627	120.024	0.627	192.547	3.158	307.93	3.119
127.764	0.652	122.65	0.652	193.033	3.285	304.21	3.239
129.906	0.677	125.08	0.677	194.58	3.411	274.538	3.358

132.208	0.702	127.336	0.702	196.437	3.538	221.645	3.478
134.756	0.727	129.818	0.727	198.948	3.666	223.304	3.602
137.336	0.752	132.35	0.752	191.287	3.792	213.764	3.726
140.18	0.777	134.498	0.777	185.27	3.92	213.048	3.85
142.704	0.802	137.01	0.802	177.804	4.048	221.338	3.974
145.138	0.827	139.934	0.827	164.192	4.176	226.033	4.098
147.592	0.851	142.78	0.852	160.17	4.303	228.152	4.221
149.418	0.877	145.144	0.877	158.084	4.429	231.36	4.345
151.872	0.901	147.538	0.901	156.517	4.555	225.982	4.469
154.112	0.927	149.798	0.927	158.692	4.682	210.31	4.594
156.434	0.952	151.428	0.952	157.131	4.809	209.882	4.717
158.938	0.976	153.886	0.976	151.64	4.939	218.296	4.84
160.718	1.002	156.512	1.002	137.514	5.059	218.883	4.958
163.412	1.027	158.766	1.027				
166.23	1.051	160.318	1.051				
168.624	1.077	162.018	1.077				
171.202	1.102	164.926	1.102				
174.056	1.126	167.504	1.126				
175.952	1.152	170.392	1.152				
178.198	1.176	173.064	1.176				
180.76	1.201	175.418	1.201				

182.596	1.226	177.348	1.226				
184.176	1.251	179.222	1.251				
186.848	1.276	181.043	1.276				
189.624	1.301	183.025	1.301				
192.098	1.326	185.16	1.326				
194.104	1.351	187.794	1.351				
196.832	1.376	190.086	1.376				
199.388	1.401	192.306	1.401				
201.892	1.426	194.4	1.426				
203.598	1.451	196.918	1.451				
205.112	1.475	199.538	1.475				
199.278	1.496	201.764	1.5				
201.886	1.521	203.732	1.525				
204.142	1.546	198.012	1.546				
205.944	1.571	200.52	1.571				
207.656	1.596	202.97	1.596				
209.398	1.62	204.722	1.62				
210.884	1.645	206.912	1.645				
212.708	1.67	209.056	1.67				
214.672	1.695	211.168	1.695				
214.422	1.718	213.124	1.72				

208.175	1.741	214.922	1.744				
193.932	1.766	214.567	1.768				
196.16	1.791	207.606	1.791				
186.22	1.816	209.888	1.816				
187.027	1.841	212.986	1.841				
192.767	1.867	215.356	1.865				
189.214	1.89	217.682	1.89				
181.589	1.915	219.844	1.915				
178.657	1.936	222.068	1.94				
180.651	1.96	223.7	1.964				
173.623	1.986	222.59	1.988				
174.482	2.011	216.338	2.01				
176.758	2.035	208.556	2.034				
175.055	2.059	197.352	2.057				
176.613	2.082	198.552	2.082				
169.249	2.109	197.627	2.107				
167.36	2.134	195.909	2.132				
160.521	2.157	188.312	2.156				
151.544	2.183	188.698	2.181				
126.858	2.208	187.804	2.205				
78.088	2.232	187.321	2.231				

66.41	2.259	184.974	2.255				
42.335	2.285	173.708	2.28				
20.188	2.31	164.115	2.305				
11.358	2.335	161.906	2.331				
10.295	2.361	155.212	2.355				
12.997	2.383	141.863	2.379				
13.633	2.409	140.767	2.406				
9.784	2.434	123.198	2.431				
7.787	2.462	97.816	2.456				